Development/Plasticity/Repair

Neuronal Activities in the Rostral Ventromedial Medulla Associated with Experimental Occlusal Interference-Induced Orofacial Hyperalgesia

Si-Yi Mo (莫思怡),[1,2,3] Xiao-Xiang Xu (徐啸翔),[1,2,3] Shan-Shan Bai (白珊珊),[1,2,3] Yun Liu (刘云),[1,2,3] Kai-Yuan Fu (傅开元),[2,3,4] Barry J. Sessle,[5,6,7] Ye Cao (曹烨),[1,2,3] and Qiu-Fei Xie (谢秋菲)[1,2,3]

[1]Department of Prosthodontics, Center for Oral and Jaw Functional Diagnosis, Treatment and Research, School and Hospital of Stomatology, Peking University, Beijing 100081, People's Republic of China, [2]National Engineering Research Center for Oral Biomaterials and Digital Medical Devices, Beijing 100081, People's Republic of China, [3]National Clinical Research Center for Oral Diseases, Beijing 100081, People's Republic of China, [4]Center for Temporomandibular Disorders and Orofacial Pain, School and Hospital of Stomatology, Peking University, Beijing 100081, People's Republic of China, [5]Faculty of Dentistry, University of Toronto, Toronto, Ontario M5G 1G6, Canada, [6]Department of Physiology, Temerty Faculty of Medicine, University of Toronto, Toronto, Ontario M5S 1A8, Canada, and [7]Centre for the Study of Pain, University of Toronto, Toronto, Ontario M5T 1P8, Canada

The imbalanced conditions of pronociceptive ON-cells and antinociceptive OFF-cells in the rostral ventromedial medulla (RVM) alter nociceptive transmission and play an important role in the development of chronic pain. This study aimed to explore the neuroplastic mechanisms of the RVM ON-cells and OFF-cells in a male rat model of experimental occlusal interference (EOI)-induced nociceptive behavior reflecting orofacial hyperalgesia and in modified models involving EOI removal at early and later stages. We recorded the mechanical head withdrawal thresholds, orofacial operant behaviors, and the activity of identified RVM ON-cells and OFF-cells in these rats. EOI-induced orofacial hyperalgesia could be relieved by EOI removal around postoperative day 3; this effect could be inhibited by intra-RVM microinjection of the κ-opioid receptor agonist U-69593. EOI removal around postoperative day 8 did not relieve the orofacial hyperalgesia, which could, however, be reversed by intra-RVM microinjection of the NK-1 (neurokinin-1) receptor antagonist L-733060. The activity of ON-cells and OFF-cells did not change during both the initial 3 and 6 d of EOI. When EOI was removed on postoperative day 3, OFF-cell responses decreased, contributing to the reversal of hyperalgesia. When EOI lasted for 8 d or was removed on postoperative day 8, spontaneous activity and stimulus-evoked responses of ON-cell increased, contributing to the maintained hyperalgesia. In contrast, when the EOI lasted for 14 d, OFF-cell responses decreased, possibly participating in the maintenance of hyperalgesia with persistent EOI. Our results reveal that adaptive changes in the RVM were associated with orofacial pain following EOI placement and removal.

Key words: experimental occlusal interference; hyperalgesia; opioids; orofacial pain; pain modulation; rostral ventromedial medulla

Significance Statement

A considerable proportion of patients experience chronic orofacial pain throughout life despite the therapies given or removal of potential etiologic factors. However, current therapies lack effectiveness because of limited knowledge of the chronicity mechanisms. Using electrophysiological recording, combined with a behavioral test, we found that the prevailing descending facilitation in the rostral ventromedial medulla (RVM) participates in the maintenance of orofacial hyperalgesia following late removal of nociceptive stimuli, while the prevailing descending inhibition from the RVM may contribute to the reversal of orofacial hyperalgesia following early removal of nociceptive stimuli. Thus, variable clinical outcomes of orofacial pain may be associated with descending modulation, and an optimal window of time may exist in the management of chronic orofacial pain.

Received Jan. 3, 2022; revised Apr. 14, 2022; accepted May 24, 2022.

Author contributions: S.-Y.M., Y.C., and Q.-F.X. designed research; S.-Y.M. and S.-S.B. performed research; S.-Y.M., X.-X.X., S.-S.B., Y.L., K.-Y.F., B.J.S., Y.C., and Q.-F.X. analyzed data; S.-Y.M. wrote the paper.

This research was supported by the National Natural Science Foundation of China (Grant 81970955, to Y.C.), the Natural Science Foundation of Beijing Municipality (Grant 7192231, to Y.C.), and the National Natural Science Foundation of China (Grants 81771096 and 82071138, to Q.-F.X.; 81800998, to X.-X.X.; and 81870788, to K.-Y.F.).

The authors declare no competing financial interests.

Correspondence should be addressed to Ye Cao at ye.cao@bjmu.edu.cn or Qiu-Fei Xie at xieqiuf@163.com.

https://doi.org/10.1523/JNEUROSCI.0008-22.2022

Introduction

The descending pain modulatory system includes the rostral ventromedial medulla (RVM) which functions as a bidirectional pain control relay to integrate and ultimately convey descending pain facilitatory or inhibitory influences to the spinal dorsal horn and medullary dorsal horn (MDH), thus modulating nociceptive transmission (Kwon et al., 2014; Bodnar and Heinricher, 2016; Chichorro et al., 2017; Martins and Tavares, 2017). The neurons in the RVM are composed of ON-cells, OFF-cells, and NEUTRAL-cells, classified by their electrophysiological characteristics and roles in pain modulation (Heinricher et al., 1989; Fields, 2004). Pronociceptive changes in RVM neuronal response properties reflected in increased ON-cell firing and decreased OFF-cell firing contribute to enhanced dorsal horn nociceptive neuronal excitability and behavioral hypersensitivity after nerve injury (Okubo et al., 2013), peripheral neuropathy (Carlson et al., 2007; Gonçalves et al., 2007; Silva et al., 2013; Nones et al., 2017), and inflammation (Khasabov et al., 2012, 2017; Cleary and Heinricher, 2013; Tang et al., 2021).

Complex signaling cascades, including both peripheral mechanisms (Ahn et al., 2009; Salas et al., 2009; Simonic-Kocijan et al., 2013; Xu et al., 2016) and mechanisms in the CNS, such as central sensitization in the MDH (Chiang et al., 2010; Iwata et al., 2011; Cao et al., 2013a,b; Wang et al., 2014; Chichorro et al., 2017; Sessle, 2021), underlie the establishment and maintenance of chronic orofacial pain. The RVM projections to the MDH are also involved in modulating trigeminal nociceptive transmission and nociceptive behavior (Sessle et al., 1981; Shimizu et al., 2009; Bryan et al., 2012).

There has been considerable focus on modulatory mechanisms in pain states driven by persistent nociceptive afferent inputs into the CNS (Okubo et al., 2013; Chichorro et al., 2017; Nones et al., 2017; Sessle, 2021), but it is also important to study pain modulation in situations where nociceptive afferent inputs into the CNS are removed to provide insights into the processes underlying recovery from chronic pain states. We have previously established a rodent model of experimental occlusal interference (EOI)-induced orofacial hyperalgesia (Cao et al., 2009). We demonstrated that orofacial hyperalgesia becomes irreversible after $\geq$6 postoperative days following EOI placement but can be reversed within the first 6 d following EOI placement (Li et al., 2014). This EOI model simulates the not uncommon clinical situations where an occlusal interference such as an ill-fitting crown or "high" filling may result in persistent pain and the pain can be relieved by early removal of the occlusal interference (Kong et al., 2016; Qi et al., 2016; Sun et al., 2016; Lin et al., 2018). Peripheral mechanisms in the trigeminal ganglion (Xu et al., 2016), central mechanisms in the MDH (Cao et al., 2013b), and enhanced thalamic-anterior cingulate cortex (ACC) synaptic transmission (Xu et al., 2019) have been shown to contribute to maintaining the orofacial hyperalgesia induced by persistent EOI (PEOI). However, how orofacial hyperalgesia is reversed or maintained by the removal of peripheral noxious stimuli remains unclear.

In this study, we hypothesized that dynamic descending modulation from ON-cells and OFF-cells in the RVM is involved in PEOI-induced hyperalgesia and the maintenance or relief of hyperalgesia following EOI removal at different postoperative stages. Therefore, the study aimed to explore the neuroplastic changes of RVM ON-cells and OFF-cells in a rat model of EOI-induced orofacial hyperalgesia and modified models created by EOI removal at different stages.

Materials and Methods

Animals

Two hundred fifty-eight adult male Sprague Dawley rats weighing 180–200 g at the beginning of the experiments were housed in individually ventilated cages under constant temperature and humidity, and a 12 h light/dark cycle, with food and water available *ad libitum*. Of these rats, 109 were used for behavioral testing, and the remaining 148 for RVM neuron recordings. The study was performed with authorization of the Institutional Animal Care and Use Committee of Peking University (Institutional Animal Care and Use Committee #LA2019353) under the ethical guidelines recommended by the International Association for the Study of Pain. Only male rats were used, to be consistent with our previous studies (which mostly used only males to avoid estrogen effects).

Procedures for experimental occlusal interference-induced orofacial hyperalgesia

The detailed process of applying an EOI to induce orofacial hyperalgesia involves placing a crown on the right maxillary first molar (Cao et al., 2009). A sharp probe was used to remove the crown, thereby removing the EOI (REOI). Removing the EOI before postoperative day 6 results in the reversal of orofacial hyperalgesia, whereas removing the EOI after postoperative day 6 cannot prevent the development of persistent hyperalgesia (Li et al., 2014; Liu et al., 2016). The time course of EOI-induced orofacial mechanical hyperalgesia can be divided into the following two stages (Li et al., 2014; Liu et al., 2016): an initial stage (postoperative days 0–5) when EOI-induced hyperalgesia become established but is reversible; and a maintenance stage (postoperative day 6 and beyond) when hyperalgesia becomes sustained and is irreversible (Fig. 1*A*). Therefore, four animal groups were used in the behavioral experiment: one group had sham EOI (sham group), another group had persistent EOI (PEOI group; i.e., no EOI removal), a third group had the REOI on postoperative day 3 (REOI 3 d group), and a fourth group had REOI on postoperative day 8 (REOI 8 d group; Fig. 1*B*).

Behavioral testing

Behavioral testing included head withdrawal threshold (HWT) measurement and orofacial operant testing in 110 rats. The HWT assessment measures reflexive nociceptive behavioral responses, whereas the orofacial operant test records nociceptive behavior reflecting the integration of higher CNS processing of the EOI-evoked nociceptive afferent inputs (Cha et al., 2012; Abd-Elsayed et al., 2015). Mechanical hypersensitivity was tested but not other forms of hypersensitivity (e.g., thermal hypersensitivity) to simulate the clinical state of EOI-induced mechanical tenderness in the orofacial region.

Measurement of head withdrawal threshold. Ipsilateral and contralateral head withdrawal responses were evoked by mechanical stimulation of the facial skin overlying the belly of the masseter muscle on both sides of the head separately by a modified electronic von Frey anesthesiometer (BIO-EVF3, Bioseb). On days 4, 5, and 6 before the application of the EOI or cannula implantation surgery, rats were placed in the testing environment for 30 min/d to acclimatize them to the surroundings. On days 1, 2, and 3, the ipsilateral and contralateral HWTs were measured and the average of the HWTs was calculated as the ipsilateral and contralateral baseline HWTs, respectively. Details of the procedures have been described previously (Cao et al., 2009). The observer was blinded to the treatments during the whole measurement process.

Orofacial operant test. The method used for the operant test was similar to that used previously (Abd-Elsayed et al., 2015) with the Orofacial Stimulation Test System (Ugo Basile). Each animal was placed in this test system with a drinking window that allowed it to enter and acquire a reward (30% sweetened condensed milk; Nestle China) from a nipple associated with the system. The operant test included the following two stages: the first stage was four to six sessions of adaptation training over 2 weeks initially, and the second stage was the actual testing. Before each adaptation training or testing session, the rats underwent a 20 ± 1 h food-fasting period. During the adaptation, each rat was placed in the test system for 20 min to become familiar with the environment and acquire food rewards either with or without mechanical stimulation. During the testing, a mechanical stimulation module was installed

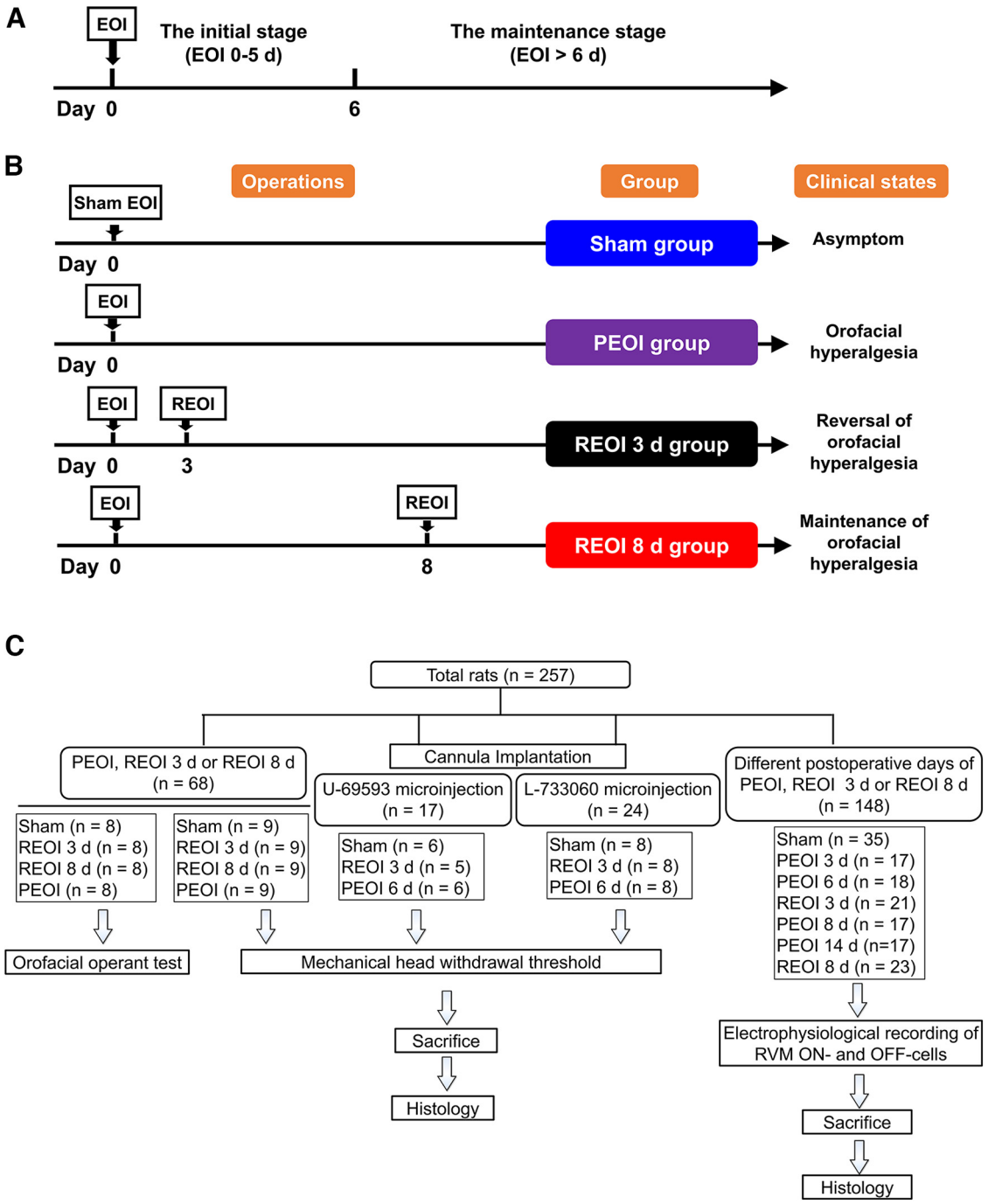

Figure 1. Three different stages in the course of orofacial hyperalgesia induced by PEOI and the establishment of four groups. ***A***, Schematic diagram of different stages in the course of PEOI-induced orofacial hyperalgesia. ***B***, Diagrammatic drawings of four EOI-related animal groups and the associated clinical states are represented. ***C***, The flowchart of experimental design and animal sizes of each experiment. The excitability of OFF-cells increased, but the activity of ON-cells did not change in the REOI 3 d group while the excitability of ON-cells increased, but the activity of OFF-cells did not change in the REOI 8 d group, so we used the KOR agonist U-69593 in the REOI 3 d group and NK-1 receptor antagonist L-733060 in the REOI 8 d group to manipulate the activity of OFF-cells and ON-cells respectively. Asymptom, Asymptomatic.

within the drinking window. The position of the drinking nipple was determined through pretrials to ensure that stimulation of the orofacial region occurred when the animal was drinking milk. Mechanical stimulation was applied to the orofacial region when the head of the rat accessed the drinking nipple. The rat was able to retract its head freely if it could not bear any pain associated with the stimulation. This method is considered to be a self-disciplined operant test (Cha et al., 2012). After 2 weeks of presurgical adaptation training, each rat was allowed 10 min to become familiar with the environment, and the rat was allowed to drink milk for the subsequent 10 min freely. Through a built-in infrared apparatus, the system automatically recorded the events as the head of the rat accessed the drinking nipple. These events were analyzed by Oro Software (Ugo Basile). The observer was blinded to the treatments of rats during the whole measurement process.

Cannula implantation and drug microinjections

κ-Opioid receptor (KOR) agonists have been found to directly inhibit the activity of OFF-cells and NEUTRAL-cells (Meng et al., 2005; Winkler et al., 2006). Furthermore, several studies have shown that neurokinin-1 (NK-1) receptor antagonists can modulate the excitability of

ON-cells in the RVM and are involved in acute or chronic inflammatory hyperalgesia (Dénes et al., 2007; Pacharinsak et al., 2008; Khasabov et al., 2012, 2017; Cleary and Heinricher, 2013). Thus, KOR agonists or NK-1 receptor antagonists were microinjected into the RVM to manipulate the function of OFF-cells or ON-cells, respectively.

Cannula implantation surgery was performed after adaptation and baseline HWT measurement. Rats were anesthetized and placed into a stereotaxic apparatus. A skin incision was made, and a small bone plug was removed from the skull so that a guide cannula [outer diameter (o.d.), 0.56 mm; inner diameter (i.d.), 0.38 mm] could be lowered into the RVM with the following stereotaxic coordinates: anteroposterior (AP), −10.92 mm from the bregma; dorsoventral (DV), +10 mm from the cranial surface; length (L), 0 mm from the midline. Then, the guide cannula was fixed in place with dental cement. To prevent blocking of the guide cannula, a dummy cannula was inserted and secured in position until the time of injection. The skin incision was sutured with 4–0 silk thread. Animals were allowed to recover for 7 d before any further experimentation.

All drugs were microinjected with an inserted injection cannula (o.d., 0.36 mm; i.d., 0.20 mm) that protruded for 0.5 mm beyond the tip of the guide cannula under isoflurane inhalation anesthesia (induction, 4%; maintenance, 1.5–2%). The injection tube was attached to a Hamilton microsyringe (RWD Life Science) via PE-10 polyethylene tubing within the guide cannula. A microsyringe pump (model 310 plus, KD Scientific) was used to deliver drugs in a volume of 0.5 µl for 2 min at the doses specified below (see Experimental design section). Another 2 min delay was ensured before retraction of the injection tube to allow for complete drug diffusion. At the end of the experiment, "direct blue" dye (0.5 µl) was injected to verify the injection sites and ranges. Only rats with the tip of a cannula correctly placed in the RVM were used. The diffusion ranges of the drugs indicated by direct blue dye were within the RVM area. No obvious tissue damage was found around the injection range in the histologic sections.

Neuron recording and stimulation procedures

Initially, rats were anesthetized with urethane (1 g/kg) injection intraperitoneally. Then, the rat was placed into a stereotaxic apparatus (model 940, David Kopf Instruments) with its ventral surface resting on a feedback-controlled heating blanket to maintain physiological core body temperature. After infiltration anesthesia under the shaved scalp with lidocaine and exposure of the cranium, a small craniotomy was made ~10 mm posterior to the bregma, and the dura was removed to allow for access to the RVM with a recording microelectrode.

In accordance with several earlier studies, recordings of neurons in the RVM were made in general anesthetized rats (Fields, 2004; Ossipov et al., 2014; Chichorro et al., 2017; Nones et al., 2017). In animals initially induced using urethane, we waited at least 2.5 h before starting electrophysiological recording to discriminate the neurons by withdrawal reflexes of tail pinches in lightly anesthetized rats.

Stereotaxic coordinates used for RVM neuronal firing activity recordings were as follows: AP −9.9 to −11.5 mm from the bregma; DV, +9.4 to +10.6 mm from the cranial surface; L, −1.1 to 1.1 mm from the midline. During the recording period, an additional dose of urethane (200–300 mg/kg/h, i.p.) was administered to maintain anesthesia. A stainless steel microelectrode (tip impedance, 10–18 MΩ at 1 kHz; A-M Systems) was then lowered into the RVM by a direct drive micropositioner (model 2662, David Kopf Instruments) in 10 µm steps. RVM neuronal firing activity was recorded extracellularly and then amplified, filtered, and displayed on a storage oscilloscope using the Pclamp 11 Software Suite (Molecular Devices). The waveforms of individual neurons were distinguished from each other offline by event detection and event sorting using Clampfit 11 software (Molecular Devices).

The RVM neurons were first functionally classified as ON-cells, OFF-cells, or NEUTRAL-cells according to their ongoing spontaneous discharge activity, their responses to tail pinches and relevant tail flicks after tail pinches (Silva et al., 2013; Khasabov et al., 2015, 2017; Salas et al., 2016). Then, their responses evoked by two types of stimuli to the shaved facial skin overlying the masticatory muscle were recorded. One type of stimulus was applied by using von Frey filaments (60, 100, and 180 × *g* forces in ascending order), and the other modality was pinch stimulation, which was applied by smooth forceps (with a force that could cause pain when applied to the experimenter's skin). The von Frey filaments exert mechanical force on superficial tissues, whereas pinch forceps may stimulate both superficial and deep tissues (Takahashi et al., 2005). OFF-cells were tested with a von Frey filament force of only 180 × *g* and pinch stimulation because we found in preliminary experiments that they did not always respond significantly to von Frey filament forces of 60 and 100 × *g*. The head withdrawal latency or threshold could not be measured by mechanical stimulation to the orofacial region at the same time as the electrophysiological recordings because the rat head was fixed in a stereotaxic apparatus.

All neurons classified as ON-cells responding to tail pinches also responded with increased activity evoked by von Frey filaments or pinch stimulation applied within the facial skin overlying the masseter muscles in our experiments, whereas ~90% of OFF-cells responding with decreased activity to tail pinches also responded with decreased activity to the von Frey filament and pinch stimulation applied to this facial region. Only the neurons that responded to the stimulus applied to the facial skin with an obvious increase (>20% above baseline level) in discharge rate (i.e., ON-cells) or a decrease (>20% below baseline level) in discharge rate (i.e., OFF-cells) and whose signal-to-noise ratio of action potentials was ≥3:1 were further studied. NEUTRAL-cells, consistent with earlier studies (Fields, 2004; Cleary and Heinricher, 2013; Silva et al., 2013; Khasabov et al., 2017), displayed no or only a very small (<10%) alteration in discharge rates by noxious stimulation to the facial region and were not studied further.

At the end of each recording session, an electrolytic lesion (50 µA for 30 s) was made at the recording site. Animals were perfused with 4% paraformaldehyde, and the brainstems were extracted. Histologic verifications of the recording sites were made in 50 µm sections of the brainstems. Subsequently, reconstruction graphs of recording sites were drawn by referring to the standard brain atlas of the rat (Paxinos and Watson, 2009).

Experimental design

The experimental design and animal sizes of each experiment are shown in Figure 1*C*. For measurement of HWTs, 36 rats were randomly assigned into sham, REOI 3 d, REOI 8 d, and PEOI groups ($n = 9$ for each group). For the orofacial operant test, another 32 rats were randomly divided into the following four groups ($n = 8$ for each group): sham, REOI 3 d, REOI 8 d, and PEOI rats. Total contact time (TCT) refers to the total amount of time that the head of the rat accessed the drinking nipple during the testing session, and the TCT over a 10 min experimental session was used as an orofacial operant behavioral parameter. The orofacial operant tests were performed on days 1, 3, and 5 before the application of the EOI (baseline), and on days 3, 6, 9, and 14 after the application of the EOI; these time points were selected to be close to those used for the HWT measurements. Because this test requires a food-fasting period before each testing session, it was considered inappropriate to perform the behavioral testing too frequently. Therefore, the testing time points in the orofacial operant test were selected to be close to the time points used for determining the HWTs, which were measured before and after drug microinjection within 1 d.

For the 42 rats that received cannula implantation surgery to manipulate the function of OFF-cells or ON-cells, the HWTs of these rats in different groups were measured at the following time points: precannula implantation surgery (baseline); pre-drug microinjection (pre); after vehicle or artificial CSF (aCSF) microinjection; and at 30 min and 120 min after drug microinjection on postoperative day 6 or 14. Eighteen of these rats were randomly divided into sham, REOI 3 d, and PEOI groups ($n = 6$ for each group) and received microinjection of a vehicle [10% (w/v) 2-hydroxy-β-cyclodextrin] or the KOR agonist U-69593 on postoperative day 6. One of these 18 rats was excluded before any microinjection experiment because of abnormal behavior. The KOR agonist U-69593 (1 mg/ml; Sigma-Aldrich) was dissolved in 10% (w/v) 2-hydroxy-b-cyclodextrin for microinjection (Ackley et al., 2001); this dose is effective in producing pronociceptive effects (Foo and Helmstetter, 2000; Meng et al., 2005). The other 26 rats were

randomly divided into sham, REOI 8 d, and PEOI groups ($n = 8–9$ for each group) and received microinjection of aCSF or NK-1 receptor antagonist L-733060 on postoperative day 14. L-733060 (10 mg/ml; Tocris Bioscience) was diluted in aCSF containing 147 mM NaCl, 3.0 mM KCl, 0.8 mM $MgCl_2$, 1.2 mM $CaCl_2$, 2.0 mM NaH_2PO_4, and 2.0 mM Na_2HPO_4; this dose is effective in reversing NK-1-related nociceptive responses (Chai et al., 2012; Khasabov et al., 2012). Data from 2 of these 26 rats were excluded from the statistical analysis because of the histologic analysis, which suggested a possible diffusion to adjacent nuclei (e.g., the dorsal nucleus reticularis gigantocellularis and raphe pallidus nucleus).

Another 148 rats were used in extracellular single-unit electrophysiological recording experiments. Activities of neurons in the RVM were recorded at different time points in the following groups: (1) on postoperative days 3, 6, 8, and 14 of the PEOI rats; (2) on postoperative day 6 of the REOI 3 d rats; (3) on postoperative day 14 of the REOI 8 d rats; and (4) the sham rats. The spontaneous firing rate of the RVM neuron was determined by recording its ongoing basal activity over the 1–2 min period before any stimulus. The mean firing rate during the consecutive 20 s before any stimulation of an RVM ON-cell or OFF-cell was counted as the spontaneous discharge rate of the cell. Their activities were recorded after von Frey and pinch stimuli (see above), which lasted for 3 s (ON-cells) and 7 s (OFF-cells), respectively. An interval of at least ≥1 min was ensured between two consecutive stimulations to allow for the recovery of neuronal activity. A change in the stimulus-evoked neuronal activity, defined as the response of ON-cell or OFF-cell, was calculated by subtracting the spontaneous discharge rate that occurred before each stimulus from the stimulus-evoked discharge rate throughout the stimulation duration (3 s for ON-cells or 7 s for OFF cells; Silva et al., 2013; Khasabov et al., 2017). Only the activity of one or two neurons was recorded and studied continuously for each rat.

Statistical analyses

Statistical analyses were performed using SPSS version 20.0 (SPSS). All data are presented as the mean ± SEM. HWT (in grams) of ipsilateral and contralateral masseter muscles and TCT (in seconds) in different groups were compared using three-way or two-way repeated-measures ANOVA followed by the *post hoc* Bonferroni's test, respectively. For neuronal firing activity recordings, the spontaneous activities and responses of RVM ON-cells and OFF-cells expressed as firing rates were compared using one-way ANOVA for comparison among different groups; all comparisons were followed by the *post hoc* Bonferroni's test for multiple comparisons.

Results

Nociceptive behavioral changes associated with EOI placement and removal

To evaluate the different nociceptive outcomes by removing the EOI at different stages, we compared the HWTs and TCTs in the sham, REOI 3 d, REOI 8 d, and PEOI rats after EOI application (see above). EOI was found to induce orofacial mechanical hyperalgesia that was reflected in a reduced HWT related to orofacial mechanical stimulation of the skin overlying the left or right masseter muscle (which were contralateral and ipsilateral to the EOI, respectively); the presence of the hyperalgesic state related to orofacial mechanical stimulation was verified by an orofacial operant behavioral test reflected in a depressed TCT.

Measurements of the HWT were performed on days 1, 2, and 3 before EOI application (baseline) and on days 1, 3, 5, 7, 9, 14, and 21 in the sham, REOI 3 d, REOI 8 d, and PEOI rats after EOI application (Fig. 2*A*,*B*). The HWTs related to each of the two different orofacial stimulation sites (ipsilateral, contralateral) showed no significant difference between them at each time point in all groups with no significant main effect of the factor of the testing site ($F_{(1,78)} = 0\ 0.671$, $p = 0.415$). There was a significant main effect of the factors of time ($F_{(4.501,351.076)} = 114.201$, $p = 0.000$) and EOI treatment ($F_{(3,78)} = 107.432$, $p = 0.000$), as well as significant interaction of the factors of time and EOI treatment ($F_{(13.503,351.076)} = 41.412$, $p = 0.000$, three-way repeated-measures ANOVA; Fig. 2*C*). The HWTs showed no significant change during the whole experimental process in the sham group. The significantly reduced HWTs started on day 1, peaked on day 7, and were sustained until the end of the experiment (on day 21) in both the PEOI group and REOI 8 d group ($p = 0.000$ for days 1, 3, 5, 7, 9, 14, and 21 vs baseline, respectively; Fig. 2*C*). The significantly reduced HWTs in the REOI 3 d group peaked on day 3 ($p = 0.000$ for days 1, 3, and 5, $p = 0.001$ for day 7, respectively, compared with baseline; Fig. 2*C*) and had recovered to baseline level by day 9 ($p = 0.365$ for day 9, $p = 1.000$ for days 14 and 21, respectively, compared with baseline; Fig. 2*C*). There was no significant difference in HWTs between the PEOI group and the REOI 8 d group at each time point ($p > 0.05$ for all time points).

The orofacial operant test noted above was also performed on days 1, 3, and 5 before the EOI application (baseline) and on days 3, 6, 9, and 14 after the EOI application in the sham, REOI 3 d, REOI 8 d, and PEOI rats (Fig. 2*D–F*). There was significant main effect of the factors of time ($F_{(4,80)} = 12.126$, $p = 0.000$) and EOI treatment ($F_{(3,20)} = 21.653$, $p = 0.000$) as well as significant interaction between the two factors ($F_{(12,351.076)} = 3.695$, $p = 0.000$, two-way repeated-measures ANOVA; Fig. 2*G*). The TCTs showed no significant change during the whole experimental process in the sham group. TCTs of the rats were lowest at day 3 ($t_{(14)} = 28.461$, $p = 0.001$) and had recovered by day 6 ($p = 1.000$ for days 6, 9, and 14 vs baseline, respectively; Fig. 2*G*) in the REOI 3 d group. But TCTs of the rats decreased from day 3 until day 14 in both the PEOI group ($p = 0.000$ for days 6, 9, and 14 vs baseline, respectively,) and REOI 8 d group ($p = 0.000$ for days 6, 9, and 14 vs baseline, respectively; Fig. 2*G*).

Both behavioral tests were thus consistent in revealing the reversal of orofacial mechanical hyperalgesia after the EOI was removed at day 3 in the initial stage and showed that the chronification of hyperalgesia occurred at approximately day 8 after the EOI application and that maintenance of hyperalgesia was not driven by persistent EOI-evoked nociceptive afferent input since the EOI had been removed before the start of the maintenance stage.

U-69593 inhibited the reversal of orofacial hyperalgesia after EOI removal in the initial stage

To explore the role of the RVM in the reversal process of orofacial mechanical hyperalgesia after the removal of EOI in the initial stage, another experimental procedure was conducted; the KOR agonist U-69593 was microinjected into the RVM, and any changes in orofacial hyperalgesia were assessed on postoperative day 6 of the sham, PEOI, and REOI 3 d groups (Fig. 3*A*).

U-69593 is considered to selectively inhibit the function of OFF-cells, thereby facilitating nociceptive transmission (Meng et al., 2005; De Felice et al., 2011). The microinjection sites were histologically verified within the RVM (Fig. 3*B*). The HWTs related to the ipsilateral and contralateral orofacial stimulations showed no significant difference between them at each time point in all groups, with no significant main effect of the factor of the testing site ($F_{(1,28)} = 0\ 0.827$, $p = 0.371$, three-way repeated-measures ANOVA) or interaction between the factors of time and testing site ($F_{(4,112)} = 0\ 0.820$, $p = 0.356$; Fig. 3*C*). There was, however, a significant main effect of the factors of

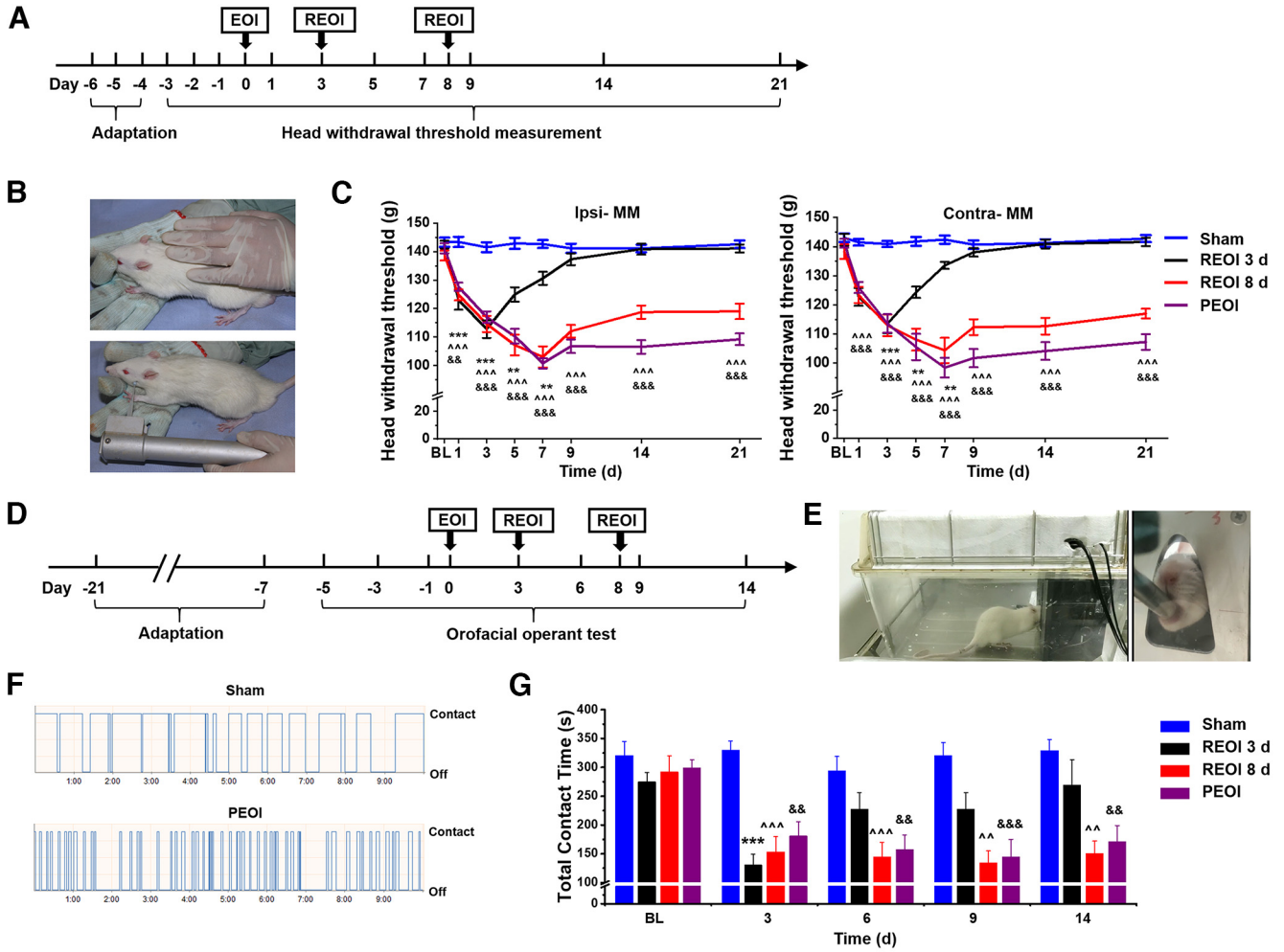

Figure 2. Orofacial hyperalgesia was reversed, maintained, or persisted in REOI 3 d, REOI 8 d, or PEOI groups, respectively. ***A***, Schematic diagram of the experimental time course of HWT measurements. Adaptation: on days 4, 5, and 6 before the EOI application, rats were placed in the testing environment 30 min/d. ***B***, Rats were comforted in the experimenter's palm; mechanical stimulation was applied to the orofacial site to measure the HWTs. ***C***, HWTs related to mechanical stimulation of ipsilateral and contralateral orofacial sites (masseters; $n = 9$ in each group) at different time points in the sham, REOI 3 d, REOI 8 d, or PEOI groups. Baseline data were acquired by measuring the average HWT for 3 consecutive days before the EOI application. ***D***, Schematic diagram of the experimental time course of orofacial operant tests. Adaptation: on days 7–21 before the EOI application, rats were placed in the testing environments for 20 min/d to acclimatize them to the surroundings. ***E***, Rats were in the testing environment and drink milk through the drinking window. ***F***, Two representative traces show the automatic recordings of drinking behavior for 10 min of a sham rat (upper trace) and a rat following EOI application (lower trace). ***G***, TCTs ($n = 8$ in each group) at different time points in the sham, REOI 3 d, REOI 8 d, or PEOI groups. Baseline data were acquired by measuring the average TCTs of three tests before the EOI application. All values are presented as the mean ± SEM. $^{**}p < 0.01$, $^{***}p < 0.001$, REOI 3 d group versus the sham group. $\wedge\wedge p < 0.01$, $\wedge\wedge\wedge p < 0.001$, REOI 8 d group versus the sham group. $\&\& p < 0.05$, $\&\&\& p < 0.001$, PEOI group versus the sham group. Three-way or two-way repeated-measures and multivariate ANOVAs were conducted, followed by *post hoc* Bonferroni's test. Ipsi-MM, Ipsilateral masseter muscle; Contra-MM, contralateral masseter muscle; BL, baseline.

time ($F_{(4,112)} = 42.195$, $p = 0.000$, three-way repeated-measures ANOVA) and EOI treatment ($F_{(2,28)} = 86.407$, $p = 0.000$) as well as significant interaction between the factors of time and EOI treatment ($F_{(8,112)} = 18.461$, $p = 0.000$; Fig. 3*C*). Behavioral testing indicated that the HWTs in the sham rats also showed no significant change during the whole experimental procedure. The HWTs were significantly reduced before drug microinjection on postoperative day 6 in both the REOI 3 d ($t_{(8)} = 5.422$, $p = 0.002$ for ipsilateral HWTs, $p = 0.000$ for contralateral HWTs) and PEOI groups ($t_{(10)} = 4.950$, $p = 0.000$ for both ipsilateral and contralateral HWTs) compared with the HWTs at baseline (Fig. 3*C*). No significant difference was found in the HWTs after vehicle (2-hydroxy-β-cyclodextrin) microinjection in both the REOI 3 d group ($t_{(8)} = 5.389$, $p = 0.001$ for ipsilateral HWTs, $p = 0.000$ for contralateral HWTs) and the PEOI group ($t_{(10)} = 4.919$, $p = 0.001$ for ipsilateral HWTs, $p = 0.000$ for contralateral HWTs) compared with the HWTs before drug microinjection (Fig. 3*C*). The HWTs were further reduced at 30 min after U-69593 microinjection ($t_{(8)} = 6.032$, $p = 0.018$ for ipsilateral HWTs, $p = 0.010$ for contralateral HWTs; Fig. 3*C*) and recovered partially at 120 min after U-69593 microinjection ($t_{(8)} = 6.955$, $p = 0.016$ for ipsilateral HWTs, $p = 0.631$ for contralateral HWTs; Fig. 3*C*) on postoperative day 6 of the REOI 3 d group compared with the HWTs after vehicle microinjection. However, on postoperative day 6 of the PEOI group, there was neither a significant difference in the HWTs at 30 min after U-69593 microinjection compared with the HWTs after vehicle microinjection ($t_{(10)} = 6.169$, $p = 0.085$ for ipsilateral HWTs, $p = 1.000$ for contralateral HWTs; Fig. 3*C*) nor a significant difference in the HWTs at 120 min compared with the HWTs at 30 min after U-69593 microinjection ($t_{(10)} = 6.286$, $p = 0.087$ for ipsilateral HWTs, $p = 1.000$ for contralateral HWTs; Fig. 3*C*). These results suggest that a pronociceptive effect of U-69593 occurred on postoperative day 3 in blocking the reversal of orofacial hyperalgesia after EOI

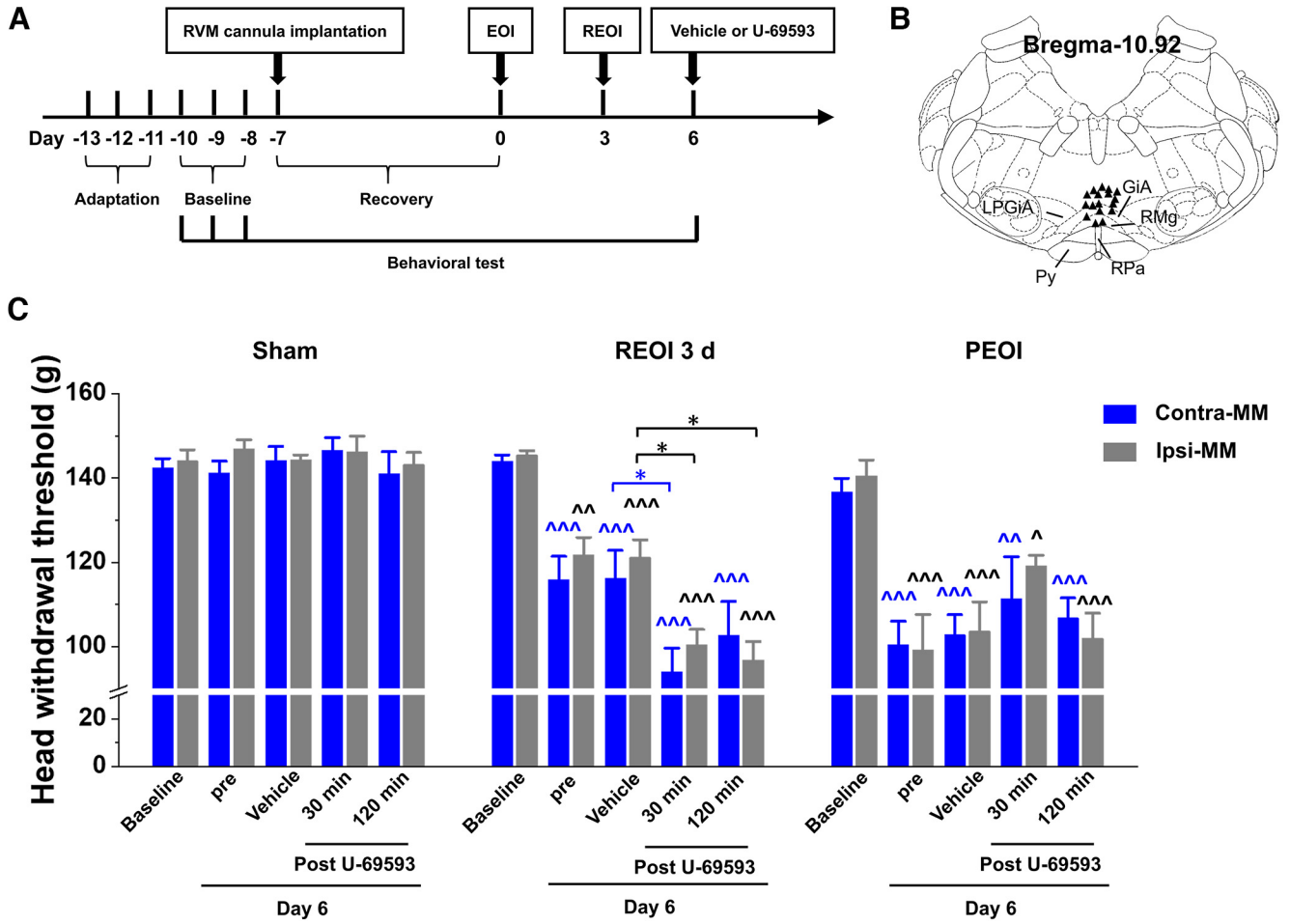

Figure 3. Effects of κ-opioid receptor agonist U-69593 on orofacial hyperalgesia induced by PEOI and REOI 3 d in the initial stage. ***A***, Schematic diagram of the experimental process and time points of HWT measurements. Adaptation: on days 11, 12, and 13 before the EOI application, rats were placed in the testing environment for 30 min/d and were comforted in the experimenter's palm. Baseline data were acquired by measuring the average HWTs on days 8, 9, and 10 before EOI application. The RVM cannula was implanted on day 7 before EOI application followed by a recovery period of 7 d. EOI was applied and then removed on postoperative day 3 or applied without removal. Vehicle or U-69593 was microinjected into the RVM on postoperative day 6. ***B***, Histologically verified microinjection sites within RVM are indicated as black triangles. The image shows a cross section of the medulla that is adapted from the stereotaxic atlas of Paxinos and Watson (2009) with permission. RMg, Nucleus raphe magnus; GiA, nucleus gigantocellularis pars α; LPGiA, lateral paragigantocellularis nucleus pars α; Py, pyramidal tract. ***C***, HWTs related to mechanical stimulation of ipsilateral and contralateral orofacial sites (masseters) were measured before surgery (baseline), before drug microinjection (pre), after vehicle microinjection, and at 30 and 120 min after U-69593 microinjection on postoperative day 6 ($n = 6$ for each group). The values are presented as the mean ± SEM. ^$p < 0.05$, ^^$p < 0.05$, ^^^$p < 0.001$, the HWT at this time point versus the baseline HWT; *$p < 0.05$. There was no significant difference between the HWTs at 30 or 120 min after L-733060 microinjection and the HWTs pre-drug microinjection. Three-way repeated-measures ANOVA, followed by *post hoc* Bonferroni's test. Ipsi-MM, Ipsilateral masseter muscle; Contra-MM, contralateral masseter muscle.

removal, while no pronociceptive effect occurred in the orofacial hyperalgesia with persistence EOI in the initial stage.

L-733060 reversed the maintenance of orofacial hyperalgesia following EOI removal around postoperative day 8

Similarly, to study the role of the RVM in the maintenance of orofacial mechanical hyperalgesia after removing the EOI around postoperative day 8, the NK-1 receptor antagonist L-733060 was microinjected into the RVM since it has been documented to modulate ON-cell excitability and suppress hyperalgesia (Dénes et al., 2007; Cleary and Heinricher, 2013; Khasabov et al., 2017). Any changes induced by L-733060 in orofacial hyperalgesia were assessed on postoperative day 14 in the sham, REOI 8 d, and PEOI groups (Fig. 4*A*). The microinjection sites of rats included in the analyses were histologically verified within the RVM (Fig. 4*B*).

The HWTs related to the ipsilateral and contralateral orofacial stimulations showed no significant difference between them at each time point in all groups, with no significant main effect of the factor of the testing site ($F_{(1,40)} = 0$ 0.580, $p = 0.451$, three-way repeated-measures ANOVA) or the interaction between the factors of time and testing site ($F_{(4,160)} = 0$ 0.493, $p = 0.741$; Fig. 4*C*). There was a significant main effect of the factors of time ($F_{(4,160)} = 69.919$, $p = 0.000$, three-way repeated-measures ANOVA) and EOI treatment ($F_{(2,40)} = 76.785$, $p = 0.000$) as well as significant interaction between the factors of time and EOI treatment ($F_{(8,160)} = 30.129$, $p = 0.000$; Fig. 4*C*). Behavioral tests in the sham rats indicated no significant change in the HWTs compared with the baseline HWTs before drug microinjection, after aCSF microinjection, or at 30 or 120 min after L-733060 microinjection on postoperative day 14. Compared with the HWTs at baseline, the HWTs were significantly reduced before drug microinjection on postoperative day 14 of both the REOI 8 d group ($t_{(14)} = 3.711$, $p = 0.000$; Fig. 4*C*) and the PEOI group ($t_{(14)} = 3.967$, $p = 0.000$), whereas the reduced HWTs were not changed after aCSF microinjection in both the REOI 8 d group ($t_{(14)} = 3.061$, $p = 1.000$; Fig. 4*C*) and the PEOI group ($t_{(14)} = 3.272$, $p = 1.000$; Fig. 4*C*) compared with

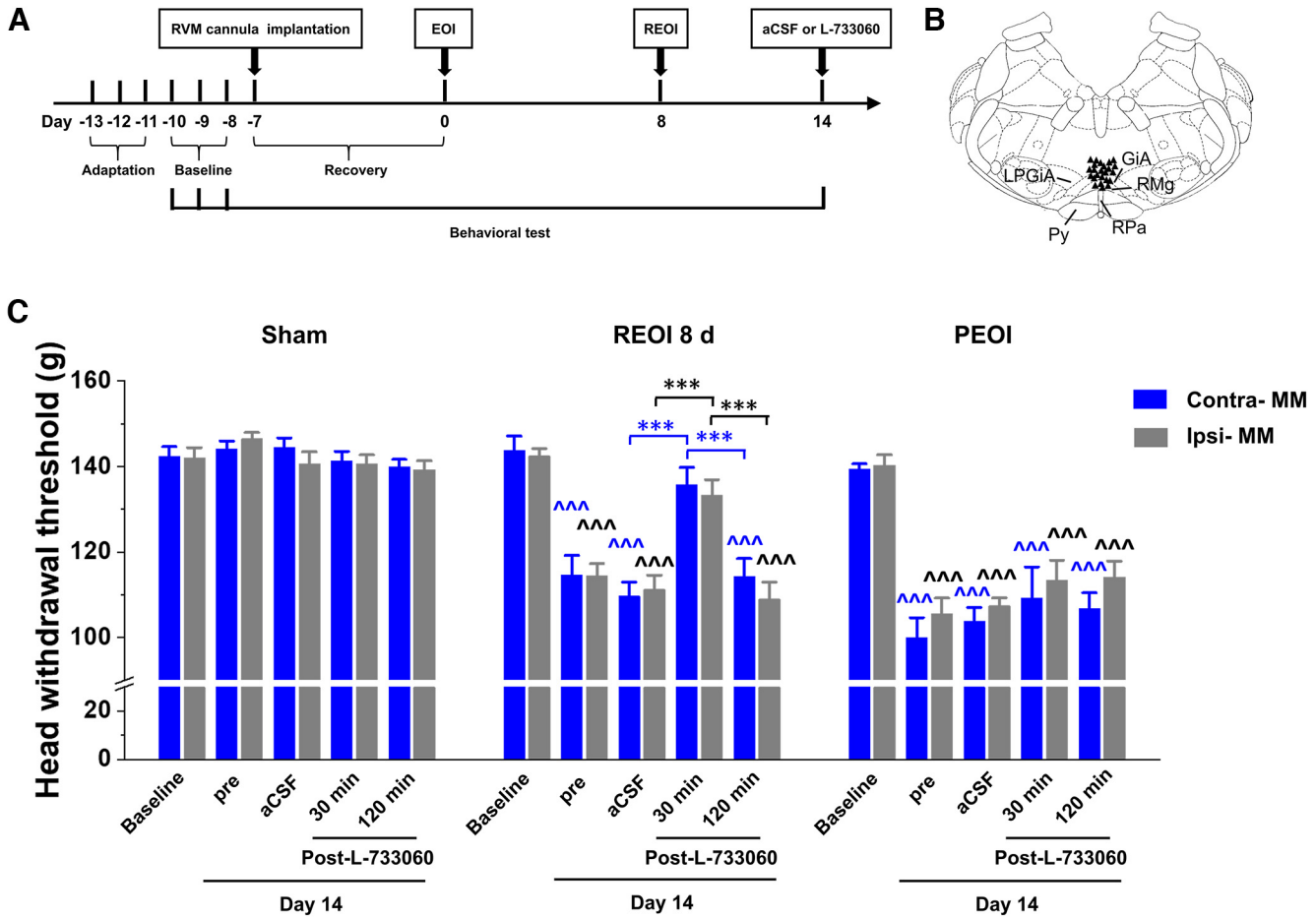

Figure 4. Effects of NK-1 receptor antagonist L-733060 on orofacial hyperalgesia induced by PEOI and REOI 8 d in the maintenance stage. ***A***, Schematic diagram of the experimental process and time points of HWT measurements. Adaptation: on days 11, 12, and 13 before the EOI application, rats were placed in the testing environment for 30 min/d and were comforted in the experimenter's palm. Baseline data were acquired by measuring the average HWTs on days 8, 9, and 10 before EOI application. The RVM cannula was implanted on day 7 before EOI application followed by a recovery period of 7 d. EOI was applied and then removed on postoperative day 3 or applied without removal. L-733060 or aCSF was microinjected into the RVM on postoperative day 14. ***B***, Histologically verified microinjection sites within RVM are indicated as black triangles. ***C***, HWTs related to mechanical stimulation of ipsilateral and contralateral orofacial sites (masseters) were measured presurgery (baseline), pre-drug microinjection, after an aCSF microinjection, and at 30 and 120 min after L-733060 microinjection on postoperative day 14 ($n = 8$ for each group). The values are presented as the mean ± SEM. ^^^$p < 0.001$, the HWT at this time point versus the baseline HWT; ***$p < 0.001$. Three-way repeated-measures ANOVA, followed by *post hoc* Bonferroni's test. Ipsi-MM, Ipsilateral masseter muscle; Contra-MM, contralateral masseter muscle.

the pre-aCSF microinjection level. In contrast, the reduced HWTs on postoperative day 14 of the REOI 8 d group were significantly reversed at 30 min postmicroinjection of L-733060 compared with the HWTs after aCSF microinjection ($t_{(14)} = 4.109$, $p = 0.000$; Fig. 4*C*) but recovered significantly at 120 min postmicroinjection compared with the HWTs at 30 min postmicroinjection of L-733060 ($t_{(14)} = 3.593$, $p = 0.000$) to the post-aCSF microinjection level ($t_{(14)} = 2.813$, $p = 1.000$). However, there was no significant difference in the HWTs post-aCSF microinjection, at either 30 or 120 min after microinjection of L-733060 on postoperative day 14 of the PEOI rats compared with the pre-aCSF microinjection level ($t_{(14)} = 3.272$, $p = 1.000$ for HWTs post-aCSF postmicroinjection vs pre-aCSF microinjection; $t_{(14)} = 4.393$, $p = 1.000$ for HWTs at 30 min postmicroinjection vs post-aCSF microinjection; $t_{(14)} = 3.843$, $p = 1.000$ for HWTs at 30 min postmicroinjection vs 120 min postmicroinjection; Fig. 4*C*). These data indicate that an antinociceptive effect of L-733060 occurred in the maintenance stage of orofacial hyperalgesia with EOI removal while no antinociceptive effect of L-733060 occurred in the maintenance stage of orofacial hyperalgesia without EOI removal.

Changes in the activity of ON-cells and OFF-cells associated with EOI placement and removal

To explore the possible involvement of RVM in behavioral changes, we recorded the spontaneous activity and evoked responses of RVM ON-cells and OFF-cells associated with EOI placement and removal (see below). The ON-cells or OFF-cells were identified according to their activity changes following tail pinch and tail flick (see Materials and Methods), and their responses evoked by the application of a noxious mechanical stimulus to the facial skin overlying the masticatory muscles were defined in terms of the changes in activity evoked by the facial mechanical stimulation. In total, 134 ON-cells and 117 OFF-cells were recorded and analyzed in the different groups of rats (sham, REOI 3 d, PEOI 3 d, PEOI 6 d, REOI 8 d, PEOI 8 d, PEOI 14 d) in the electrophysiological recordings in the study.

Changes in the activity of ON-cells and OFF-cells associated with EOI placement and removal in the initial stage

The activities of RVM neurons were assessed during the initial stage of orofacial hyperalgesia, namely on postoperative days 3 and 6 of the PEOI rats and postoperative day 6 of the REOI 3 d rats when orofacial hyperalgesia was shown to be reduced during

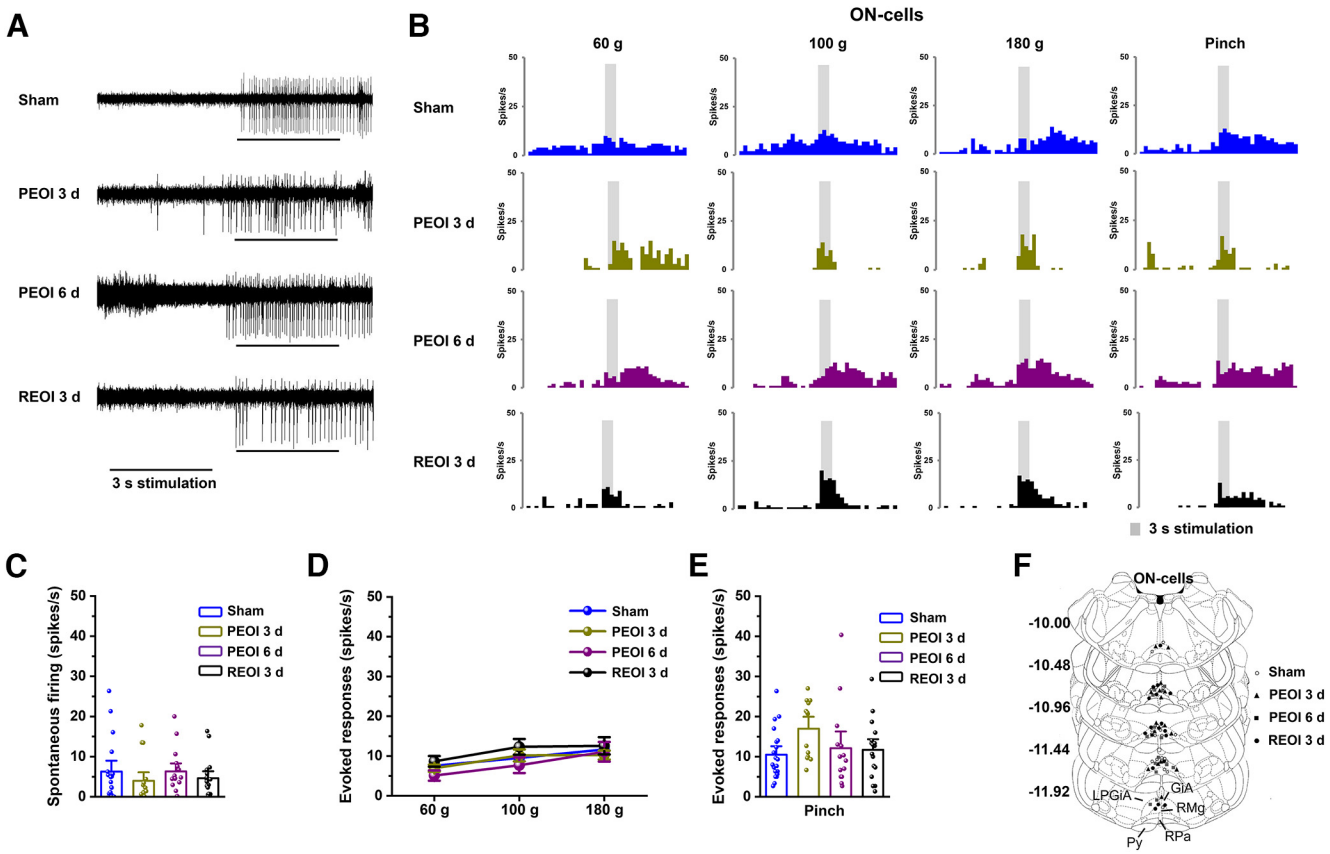

Figure 5. Spontaneous activity and responses (noxious-evoked discharge rates – spontaneous discharge rates) of ON-cells in the initial stage of orofacial hyperalgesia. ***A***, Recording examples of ON-cells in sham, PEOI 3 d, PEOI 6 d, and REOI 3 d groups. ***B***, Representative frequency histograms of firing rates of RVM ON-cells in sham (number of cells = 18), PEOI 3 d (number of cells = 16), PEOI 6 d (number of cells = 14), and REOI 3 d (number of cells = 17) groups evoked by different mechanical stimulations lasting for 3 s. Each histogram represents consecutive neural activity for 40 s. Stimulus-evoked activity over 3 s periods is indicated by a gray rectangle in each histogram. ***C–E***, Spontaneous discharge rates (***C***); the responses evoked by von Frey filament forces of 60, 100, and 180 × *g* (***D***); and the responses evoked by pinch stimulation in the four groups (***E***). ***F***, Histologic verification of the electrophysiological recording sites of ON-cells in these four groups. Images show cross sections of the medulla that were adapted from the stereotaxic atlas of Paxinos and Watson (2009) with permission. RMg, Nucleus raphe magnus; GiA, nucleus gigantocellularis pars α; LPGiA, lateral paragigantocellularis nucleus pars α; RPa, raphe pallidus nucleus; Py, pyramidal tract. The values are presented as the mean ± SEM, with one-way ANOVA, followed by *post hoc* Bonferroni's test.

the initial stage (see above); these groups of rats were respectively termed the PEOI 3 d, PEOI 6 d, and REOI 3 d groups. Since there was no statistically significant difference in neuronal activities on postoperative days 3 and 6 of the sham group, and to conserve the number of animals required for the study, we combined the animals of these two groups as a single group that was collectively termed the sham group.

Examples of ON-cell recordings in the sham, PEOI 3 d, PEOI 6 d, and REOI 3 d groups are shown in Figure 5*A*. Representative frequency histograms of firing rates of RVM ON-cells in these groups evoked by the different mechanical stimulations lasting for 3 s are presented (Fig. 5*B*). No significant difference was apparent in the spontaneous activity of ON-cells in the PEOI 3 d ($F_{(3,61)} = 0.647$, $p = 0.565$), PEOI 6 d ($F_{(3,61)} = 0.647$, $p = 1.000$), and REOI 3 d ($F_{(3,61)} = 0.647$, $p = 0.766$) groups compared with that in the sham group (one-way ANOVA; Fig. 5*C*). Also, the evoked responses of ON-cells reflected in a stimulus-induced increase in activity to von Frey filament forces of 60 × *g* ($F_{(3,61)} = 1.285$; PEOI 3 d, $p = 0.975$; PEOI 6 d, $p = 0.414$; REOI 3 d, $p = 0.858$; vs sham group, respectively, one-way ANOVA), 100 × *g* ($F_{(3,61)} = 1.064$; PEOI 3 d, $p = 0.990$; PEOI 6 d, $p = 0.828$; REOI 3 d, $p = 0.556$; vs sham group, respectively), and 180 × *g* ($F_{(3,61)} = 0.275$; for PEOI 3 d, $p = 0.912$; PEOI 6 d, $p = 0.993$; REOI 3 d, $p = 0.970$; vs sham group, respectively) or facial pinch stimulation ($F_{(3,61)} = 0.093$; PEOI 3 d, $p = 0.954$; PEOI 6 d, $p = 0.939$; REOI 3 d, $p = 0.977$; vs sham group, respectively) showed no significant difference in these rats compared with that in the sham rats (Fig. 5*D*,*E*). The locations of the recorded ON-cells were reconstructed and plotted on standardized sections (Fig. 5*F*). Neurons located outside the RVM were excluded from the analysis.

Likewise, examples of OFF-cell recordings in the sham, PEOI 3 d, PEOI 6 d, and REOI 3 d groups are shown in Figure 6*A*. Representative frequency histograms of firing rates of RVM OFF-cells in these groups evoked by the different mechanical stimulations lasting for 7 s were presented (Fig. 6*B*). No significant changes in the spontaneous activity were found in the PEOI 3 d ($F_{(3,54)} = 0.802$, $p = 0.895$, one-way ANOVA), PEOI 6 d ($p = 0.689$), and REOI 3 d group ($p = 0.956$) compared with that in the sham group (Fig. 6*C*). Also, there was no significant change in the evoked responses of OFF-cells reflected in a stimulus-induced decrease in activity to a von Frey filament force of 180 × *g* was found in the PEOI 3 d ($F_{(3,54)} = 3.582$, $p = 0.215$), PEOI 6 d ($p = 0.990$), and REOI 3 d group ($p = 1.000$) compared with that in the sham group (Fig. 6*D*). However, there were some changes in the evoked responses to facial pinch stimulation of RVM OFF-cells. Compared with the sham rats, OFF-cells responded to pinch stimulation with a reduced stimulus-induced decrease in activity in the REOI 3 d group ($F_{(3,54)} = 2.373$,

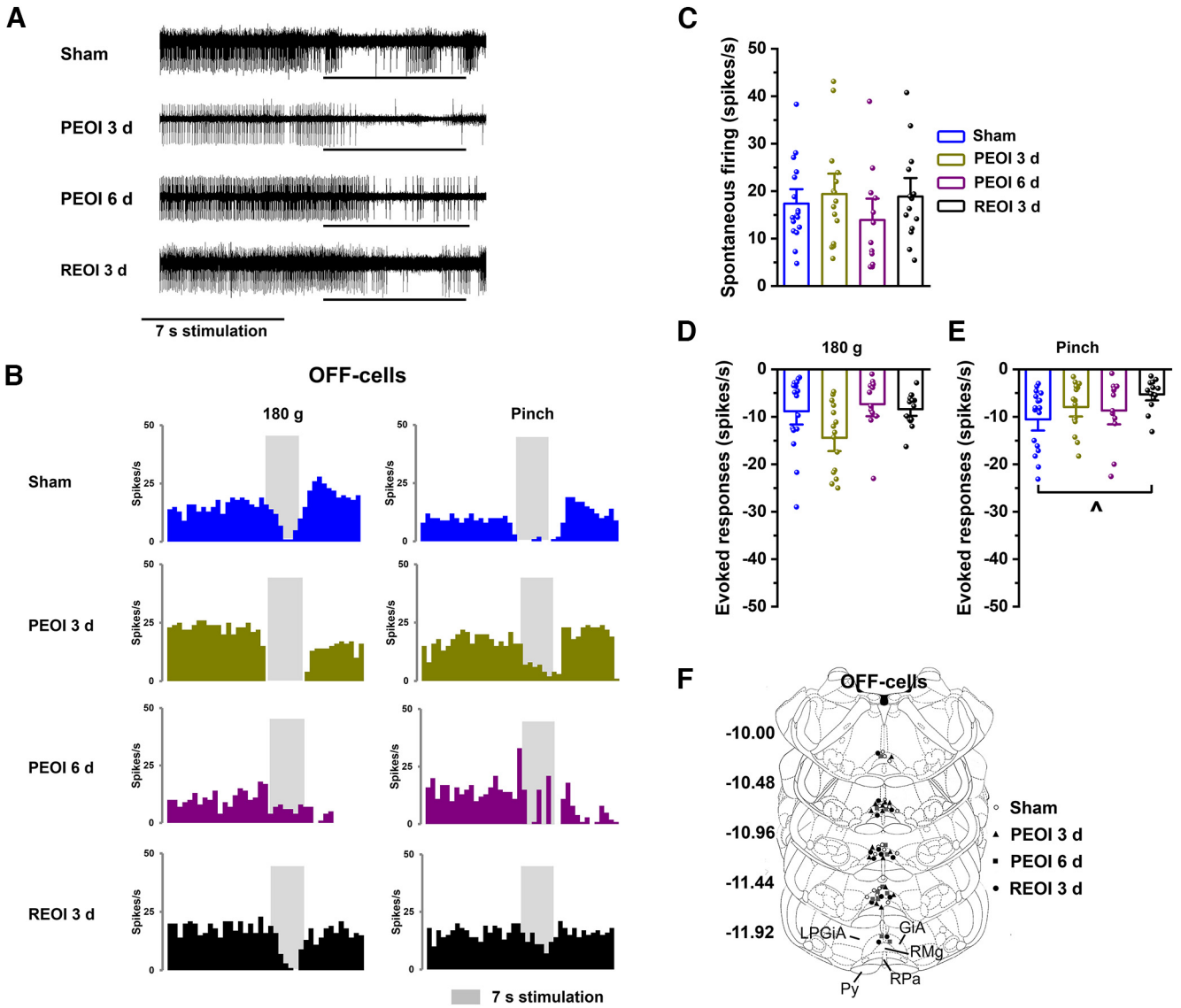

Figure 6. Spontaneous activity and responses (noxious-evoked discharge rates − spontaneous discharge rates) of OFF-cells in the initial stage of orofacial hyperalgesia. ***A***, Recording examples of OFF-cells in sham, PEOI 3 d, PEOI 6 d, and REOI 3 d groups. ***B***, Representative frequency histograms of firing rates of RVM OFF-cells in the sham (number of cells = 18), PEOI 3 d (number of cells = 15), PEOI 6 d (number of cells = 12), and REOI 3 d (number of cells = 14) groups evoked by different mechanical stimulations lasting for 7 s. Each histogram represents consecutive neural activity for 40 s. Stimulus-evoked activity over 7 s is indicated by a gray rectangle in each histogram. ***C–E***, Spontaneous discharge rates (***C***), the responses evoked by von Frey filament force of 180 × *g*, and the responses evoked by pinch stimulation in the four groups (***E***). ***F***, Histologic verification of the electrophysiological recording sites of OFF-cells in these four groups. The values are presented as the mean ± SEM. ^$p < 0.05$, REOI 3 d versus the sham group, one-way ANOVA, followed by *post hoc* Bonferroni's test.

$p = 0.029$; Fig. 6*E*); in contrast, OFF-cells showed no significant change in the evoked responses to pinch stimulation in the PEOI 3 d group ($F_{(3,54)} = 2.373$, $p = 0.491$) and the PEOI 6 d group ($F_{(3,54)} = 2.373$, $p = 0.712$; Fig. 6*E*). The locations of the recorded OFF-cells were reconstructed and plotted on standardized sections (Fig. 6*F*). Neurons located outside the RVM were excluded from the analysis.

In summary, in the initial stage of orofacial hyperalgesia, OFF-cells responded to the pinch stimuli applied to deep orofacial tissues with a reduced stimulus-induced decrease in activity after removing the EOI, while neither ON-cells nor OFF-cells showed a significant change in either spontaneous activity or stimulus-evoked responses if the EOI was left in place (i.e., with no EOI removal). These findings suggest that OFF-cells may play a major role in the processes underlying the reversal of orofacial hyperalgesia following removal of the EOI in the initial stage, while ON-cells may not. The activities of ON-cells and OFF-cells may not be significantly changed when EOI persists in the initial stage.

Changes in the activity of ON-cells and OFF-cells associated with EOI placement and removal in the maintenance stage

The activity of RVM neurons was assessed during the maintenance stages of orofacial hyperalgesia, including on postoperative days 8 and 14 of the PEOI rats and postoperative day 14 of the REOI 8 d rats; these groups of rats were respectively termed the PEOI 8 d, PEOI 14 d, and REOI 8 d groups. Since there was no statistically significant difference in neuronal activities on postoperative days 8 and 14 of the sham group, and to conserve the number of animals required for the study, we combined the animals of these two groups as a single group collectively termed the sham group.

Examples of ON-cell recordings in the sham, PEOI 8 d, PEOI 14 d, and REOI 8 d groups are shown in Figure 7*A*.

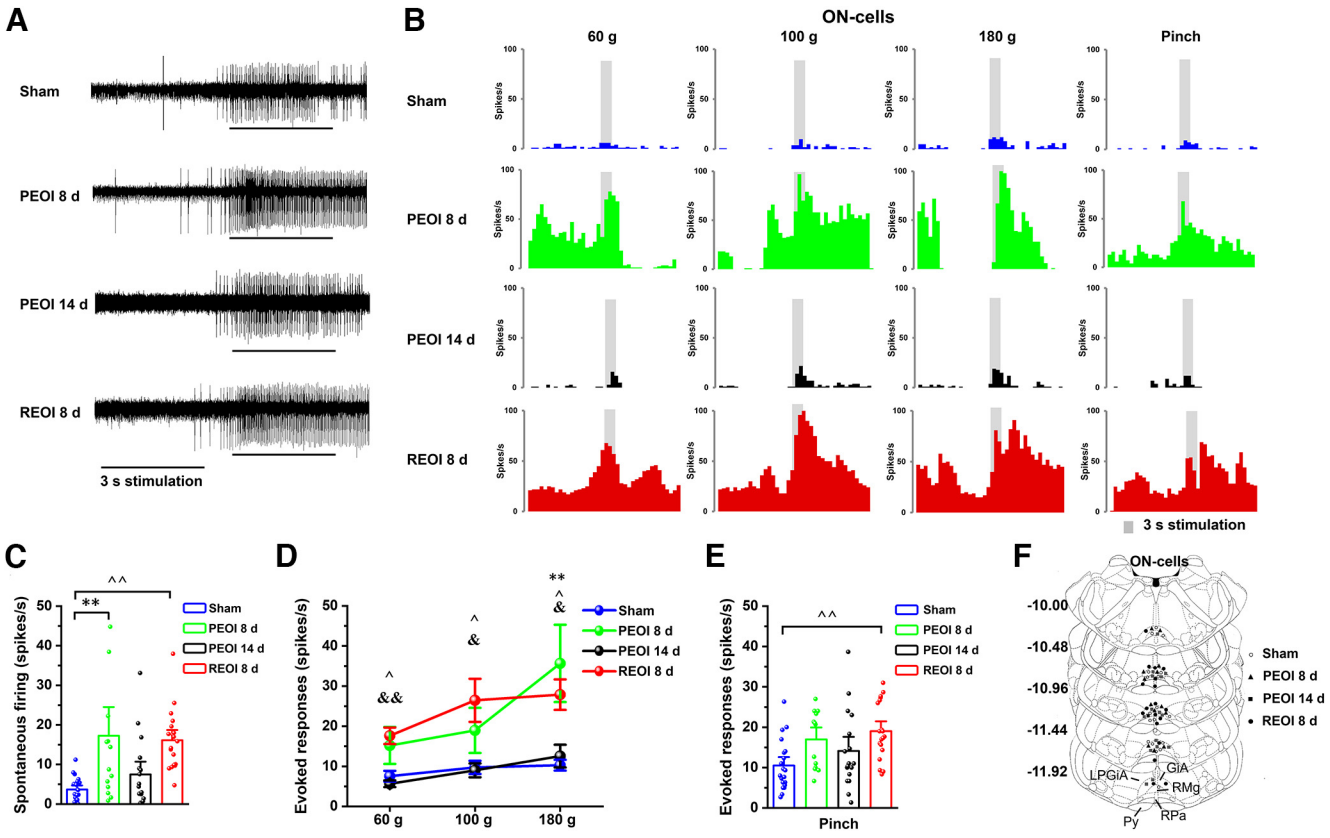

Figure 7. Spontaneous activity and responses (noxious-evoked discharge rates – spontaneous discharge rates) of ON-cells in the chronification and maintenance stages of orofacial hyperalgesia. ***A***, Recording examples of ON-cells in sham, PEOI 8 d, PEOI 14 d, and REOI 8 d groups. ***B***, Representative frequency histograms of firing rates of RVM ON-cells in the sham (number of cells = 20), PEOI 8 d (number of cells = 13), PEOI 14 d (number of cells = 17), and REOI 8 d (number of cells = 19) groups evoked by different mechanical stimulations lasting for 3 s. Each histogram represents consecutive neural activity for 40 s. Stimulus-evoked activity over 3 s is indicated by a gray rectangle in each histogram. ***C–E***, Spontaneous discharge rates (***C***); the responses evoked by von Frey filament forces of 60, 100, and 180 × *g* (***D***); and the responses evoked by pinch stimulation in the four groups (***E***). ***F***, Histologic verification of the electrophysiological recording sites of ON-cells in these four groups. The values are presented as the mean ± SEM. $^{**}p < 0.01$, PEOI 8 d versus the sham group. $^{\wedge}p < 0.05$, $^{\wedge\wedge}p < 0.01$, REOI 8 d versus the sham group. $\&p < 0.05$, $\&\&p < 0.01$, REOI 8 d versus PEOI 14 d group. One-way ANOVA, followed by *post hoc* Bonferroni's test.

Representative frequency histograms of firing rates of RVM ON-cells in these groups evoked by the different mechanical stimulations lasting for 3 s are presented in Figure 7*B*. In the PEOI 8 d group with persistent EOI, ON-cells showed an increase in the spontaneous activity ($F_{(3,66)} = 7.679$, $p = 0.002$, one-way ANOVA) and a further increase in the activity evoked by a von Frey filament force of 180 × *g* ($F_{(3,65)} = 6.982$, $p = 0.002$) compared with the sham group (Fig. 7*C*,*D*). It showed no significant change in the activity evoked by facial pinch stimulation ($F_{(3,65)} = 4.493$, $p = 0.117$) or von Frey filament forces of 60 × *g* ($F_{(3,64)} = 6.460$, $p = 0.167$) and 100 × *g* ($F_{(3,66)} = 4.930$, $p = 0.626$) in the PEOI 8 d group compared with the sham group (Fig. 7*D*,*E*). In the PEOI 14 d group, when the hyperalgesia persisted, spontaneous activity ($F_{(3,66)} = 7.679$, $p = 0.586$, one-way ANOVA) and evoked responses of ON-cells to von Frey filaments of 60 × *g* ($F_{(3,64)} = 6.460$, $p = 1.000$), 100 × *g* ($F_{(3,66)} = 4.930$, $p = 1.000$), and 180 × *g* ($F_{(3,65)} = 6.982$, $p = 1.000$) or pinch stimulation ($F_{(3,65)} = 4.493$, $p = 0.932$) had recovered to baseline values in sham rats (Fig. 7*C–E*).

In the REOI 8 d group in which RVM neuronal activity was assessed on postoperative day 14 after the EOI had been removed on postoperative day 8, there were considerable changes in the activities of ON-cells in the RVM. ON-cells showed significantly increased spontaneous activity in the REOI 8 d group compared with that in sham rats ($F_{(3,66)} = 7.679$, $p = 0.001$, one-way ANOVA) but showed no significant difference compared with those in the PEOI 14 d rats ($F_{(3,66)} = 7.679$, $p = 0.074$; Fig. 7*C*). ON-cells responded to von Frey filament forces of 60, 100, and 180 × *g* with a further increase in activity in the REOI 8 d rats compared with those in both the PEOI 14 d rats and sham rats (60 × *g*: $F_{(3,64)} = 6.460$; REOI 8 d vs sham group, $p = 0.012$; REOI 8 d vs PEOI 14 d group, $p = 0.002$; 100 × *g*: $F_{(3,66)} = 4.930$; REOI 8 d vs sham group, $p = 0.011$; REOI 8 d vs PEOI 14 d group, $p = 0.011$; 180 × *g*: $F_{(3,65)} = 6.982$; REOI 8 d vs sham group, $p = 0.025$; REOI 8 d vs PEOI 14 d group, $p = 0.016$; Fig. 7*C*,*D*). In addition, the pinch-evoked responses of ON-cells reflected in an increase in activity further increased compared with that in sham rats ($F_{(3,65)} = 4.439$, $p = 0.005$) but showed no significant difference compared with those in the PEOI 14 d rats ($F_{(3,65)} = 4.930$, $p = 0.339$; Fig. 7*E*). The locations of the recorded ON-cells were reconstructed and plotted on standardized sections (Fig. 7*F*). Neurons located outside the RVM were excluded from the analysis.

Likewise, examples of OFF-cell recordings in the sham, PEOI 8 d, PEOI 14 d, and REOI 8 d groups are shown in Figure 8*A*. Representative frequency histograms of firing rates of RVM OFF-cells in these groups evoked by different mechanical stimulations lasting for 7 s are presented in Figure 8*B*. OFF-cells showed no alteration in the spontaneous activity ($F_{(3,54)} = 2.524$, $p = 0.985$, one-way ANOVA) and evoked responses evoked by a von Frey filament force of 180 × *g* ($F_{(3,54)} = 3.010$, $p = 0.427$) or

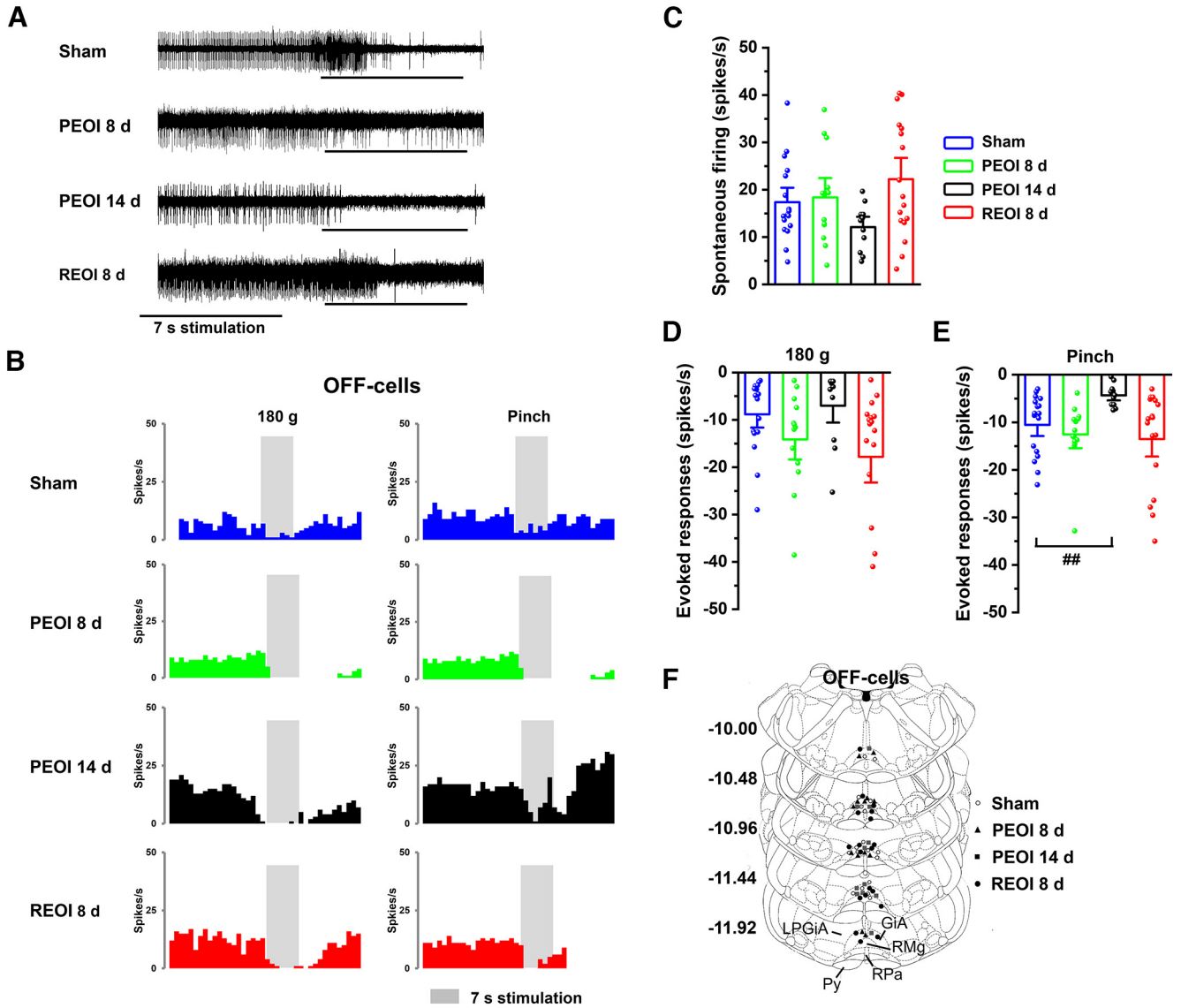

Figure 8. Spontaneous activity and responses (noxious-evoked discharge rates − spontaneous discharge rates) of OFF-cells in the chronification and maintenance stages of orofacial hyperalgesia. ***A***, Recording examples of OFF-cells in sham, PEOI 8 d, PEOI 14 d, and REOI 8 d groups. ***B***, Representative histograms of the firing rates of RVM OFF-cells in the sham (number of cells = 17), PEOI 8 d (number of cells =13), PEOI 14 d (number of cells =11), and REOI 8 d (number of cells =17) groups evoked by different mechanical stimulations lasting for 7 s. Each histogram represents consecutive neural activity for 40 s. Stimulus-evoked activity over 7 s is indicated by a gray rectangle in each histogram. ***C–E***, Spontaneous discharge rates (***C***), the responses evoked by von Frey filament force of 180 × *g* (***D***), and the responses evoked by pinch stimulation in the four groups (***E***). ***F***, Histologic verification of the electrophysiological recording sites of OFF-cells in these four groups. The values are presented as the mean ± SEM. ##$p < 0.01$, PEOI 14 d versus the sham group; one-way ANOVA, followed by *post hoc* Bonferroni's test.

facial pinch stimulation ($F_{(3,54)} = 3.836$, $p = 0.955$) in the PEOI 8 d group compared with the sham group (Fig. 8*C–E*). In the PEOI 14 d group compared with the sham rats, OFF-cells exhibited a reduced decrease in pinch-evoked activity ($F_{(3,54)} = 3.836$, $p = 0.009$, one-way ANOVA), but showed no significant change in spontaneous activity ($F_{(3,54)} = 2.534$, $p = 0.369$) and responses evoked by a von Frey filament force of 180 × *g* ($F_{(3,54)} = 3.010$, $p = 0.952$; Fig. 8*C–E*). In contrast to the changes in ON-cells, no significant alteration in the spontaneous activity ($F_{(3,54)} = 2.534$, $p = 0.335$) and stimulus-evoked responses evoked by a von Frey filament force of 180 × *g* ($F_{(3,54)} = 3.010$, $p = 0.053$) or facial pinch stimulation ($F_{(3,54)} = 3.836$, $p = 0.885$) of OFF-cells was evident in the REOI 8 d group compared with the sham group (Fig. 8*C–E*). The locations of the recorded OFF-cells were reconstructed and plotted on standardized sections (Fig. 8*F*). Neurons located outside the RVM were excluded from the analysis.

These results suggest that a transition from acute to chronic in orofacial hyperalgesia may exist. The increased spontaneous activity and evoked responses of ON-cells, rather than any significant changes in activities of OFF-cells, may play an important role in the transition of orofacial hyperalgesia induced by PEOI. The activities of ON-cells had recovered to baseline level but OFF-cells showed reduced responses evoked by pinch stimulation by day 14, which reflects a net descending inhibitory modulation. Furthermore, the increased spontaneous activity and response properties of ON-cells, rather than any significant changes in firing properties of OFF-cells, may play a vital part in maintaining orofacial hyperalgesia following late EOI removal.

Discussion

This is the first study to document the reversal and maintenance of orofacial mechanical hyperalgesia induced by EOI placement

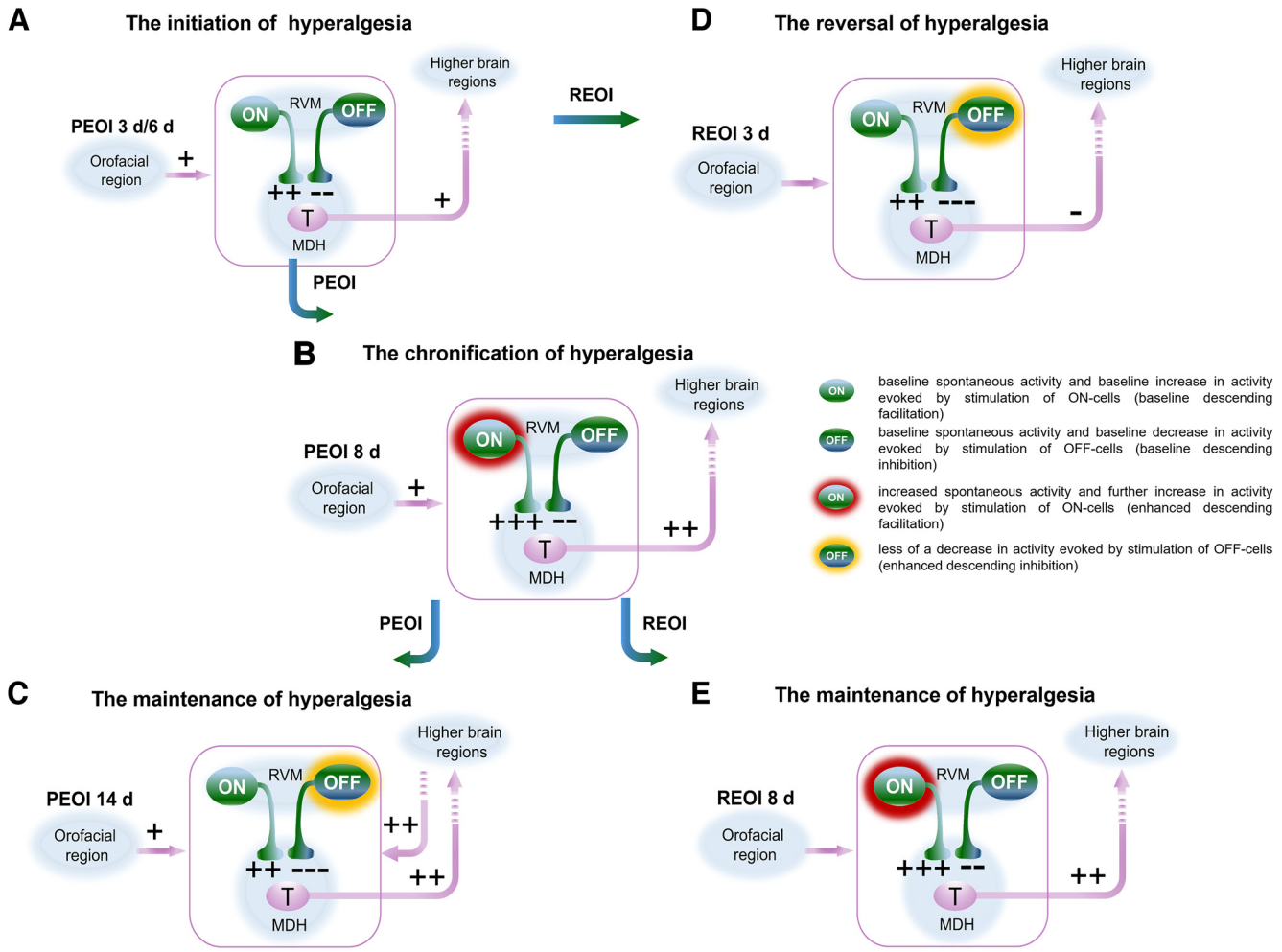

Figure 9. Schematic diagrams depicting possible modulatory actions of ON-cells and OFF-cells in the RVM on nociceptive transmission at the MDH level at different hyperalgesia stages. ***A***, The baseline descending modulatory action of ON-cells and OFF-cells in the RVM in the initiation of orofacial hyperalgesia following PEOI 3 or 6 d. ***B***, Enhanced descending facilitatory action of ON-cells on nociceptive transmission in the chronification of orofacial hyperalgesia following PEOI 8 d. ***C***, Enhanced descending inhibitory action of OFF-cells and the possible descending modulatory action of higher brain regions on nociceptive transmission in the persistence of orofacial hyperalgesia following PEOI 14 d. ***D***, Enhanced descending inhibitory action of OFF-cells on nociceptive transmission in the reversal of orofacial hyperalgesia following REOI 3 d in the initial stage. ***E***, Enhanced descending facilitatory action of ON-cells on nociceptive transmission in the maintenance of orofacial hyperalgesia following REOI 8 d in the maintenance stage. T, Transmission neurons; +, with peripheral nociceptive stimulus or enhanced nociceptive transmission; ++, baseline descending facilitatory action of ON-cells, further enhanced nociceptive transmission, or descending modulatory action of higher brain regions; ---, enhanced descending inhibitory action of OFF-cells; --, baseline descending inhibitory action of OFF-cells.

and removal in male rats and that the hyperalgesia relief or maintenance following EOI removal involves RVM neuronal activity changes in ON-cells and OFF-cells.

The findings from the two behavioral tests involving HWT measurements and an orofacial operant test were consistent with each other in revealing that PEOI-induced chronic orofacial mechanical hyperalgesia is a time-dependent process that is manifested in the following two stages: an initial stage and a maintenance stage. Both tests also showed that removing the EOI in the initial stage produced a reversal of the orofacial hyperalgesia, whereas removing the EOI in the maintenance stage did not prevent the maintenance of orofacial hyperalgesia, which is consistent with the findings of our previous studies (Li et al., 2014; Liu et al., 2016).

The behavioral findings that bilateral orofacial hyperalgesia induced by unilateral EOI are consistent with our previous documentation of such effects of an EOI (Cao et al., 2009, 2013b; Xu et al., 2016, 2019) as well as with previous studies documenting that unilateral EOI can also induce bilateral, irreversible temporomandibular joint (TMJ), masseter muscle mechanical hyperalgesia, or TMJ synovial injury (Kong et al., 2016; Qi et al., 2016; Sun et al., 2016; Lin et al., 2018). Furthermore, our findings are also consistent with those derived from other animal models in which unilateral orofacial tissue inflammation or nerve injury was shown to produce bilateral hyperalgesia or allodynia that could be accounted for by the occurrence of trigeminal central sensitization in the MDH (Ren and Dubner, 2011; Iwata and Sessle, 2019; Chung et al., 2020; Shinoda et al., 2020; Sessle, 2021).

Our findings of the activities of the ON-cells and OFF-cells concerning the time course of PEOI-induced orofacial hyperalgesia also varied in the different orofacial hyperalgesia stages. The findings of the present study suggest that descending facilitation and inhibition from the RVM are in a relatively balanced condition on postoperative days 3 and 6 (in the initial stage), with no significant change in the activities of OFF-cells and ON-cells (Fig. 9*A*). The development of orofacial hyperalgesia in the initial stage may be the result of peripheral mechanisms (Xu et al., 2016) and central sensitization in the MDH (Cao et al.,

2013b) and may not involve changes in the RVM, although other changes in descending modulatory pathways such as the RVM serotonergic pathway (Ossipov et al., 2010; Bardin, 2011), cannot be ruled out and need further study.

The neuroplastic changes in the RVM seem different between the early stage and later maintenance stage. The early maintenance stage (around postoperative day 8) may represent a critical period in the transition from acute to chronic orofacial pain induced by the EOI. Increases in the excitability of ON-cells rather than any significant changes in activities of OFF-cells compared with sham rats were found to occur during this stage, which suggests a descending facilitatory action of the RVM ON-cells that starts to become dominant. We call this transition stage a chronification stage for the sake of discussion below (Fig. 9*B*). Subsequently, descending inhibition prevails on postoperative day 14 in the later maintenance stage. The persistence of EOI-related peripheral inputs to the CNS may activate OFF-cells rather than ON-cells, which is indicative of a net inhibitory action (Fig. 9*C*).

The late occurrence of descending facilitation in the chronification stage in our model contrasts with some previous reports of the early onset of descending facilitation in the initiation of pain in other pain models (Porreca et al., 2001, 2002; Suzuki et al., 2004; Sugiyo et al., 2005). But this finding is similar to other earlier findings that descending modulation from the RVM has little role in the initiation of chronic pain but rather contributes to its maintenance (Burgess et al., 2002; Nones et al., 2017). The difference between the present findings and the earlier findings in acute pain models could be because of the modality of injury, in that the EOI-related stimulus is relatively mild compared with the stimuli used in the earlier studies (Porreca et al., 2001, 2002; Suzuki et al., 2004; Sugiyo et al., 2005). However, in the later maintenance stage, a net inhibitory action of OFF-cells was found. We speculate that the persistent nociceptive inputs could disrupt the descending analgesic system of the periaqueductal gray (PAG), which integrates information from both cortical and subcortical areas of the brain, and thus activate the OFF-cells in the RVM (Heinricher et al., 2009; Bagley and Ingram, 2020). There is also considerable evidence for a shift from descending facilitation to descending inhibition during the development of pain states induced by inflammatory injury (Terayama et al., 2000; Ren and Dubner, 2002; Cleary and Heinricher, 2013). Although the change in OFF-cell activity was insufficient to fully overcome the behavioral hypersensitivity of the maintenance stage in the present study, our observations and these earlier findings suggest that the inhibitory output of the OFF-cell acts as a compensatory adaptative process that restrains hyperalgesia (Meng et al., 2005; Carlson et al., 2007; Gonçalves et al., 2007; De Felice et al., 2011; Salas et al., 2016). Further, the maintained hyperalgesia may also be influenced by higher-level CNS regions that mediate descending modulation directly to the medullary and spinal dorsal horns, such as the ACC (López-Avila et al., 2004; Ossipov, 2009).

The present findings revealed that the enhanced inhibitory action of OFF-cells is indicative of a net antinociceptive influence contributing to the reversal of hyperalgesia if the EOI is removed in the initial stage and that this reversal process may involve an endogenous opioid-sensitive circuit (Fig. 9*D*). The KOR agonist U-69593 could aggravate orofacial hyperalgesia in rats only after removal of the EOI during the initial stage but showed no influence on the orofacial hyperalgesia in rats with persistent EOI or sham EOI. U-69593 can be either pronociceptive, through inhibiting OFF-cells directly, or antianalgesic, indirectly through both postsynaptic inhibition and presynaptic inhibition of glutamate inputs to RVM OFF-cells (Pan et al., 1997; Meng et al., 2005; Winkler et al., 2006). U-69593 has also been shown to functionally antagonize μ-opioid receptor-mediated analgesia induced from the RVM (Meng et al., 2005). Thus, the mechanisms of this pronociceptive effect of U-69593 in our experiment on inhibiting the antinociceptive influence of OFF-cells remain to be seen.

The RVM electrophysiological findings also demonstrated that an enhanced facilitatory action of ON-cells may play a vital part in maintaining orofacial hyperalgesia following EOI removal during the chronification stage around postoperative day 8 (Fig. 9*E*). Thus, the prevailing influence of the descending facilitatory action of ON-cells may result in a net facilitatory influence that reinforces trigeminal nociceptive transmission (Sugiyo et al., 2005; Salas et al., 2016). The NK-1 receptor antagonist L-733060 has been shown to suppress the enhanced excitability of ON-cells and block hyperalgesia but does not affect the excitability of ON-cells in control or sham animals (Dénes et al., 2007; Cleary and Heinricher, 2013; Khasabov et al., 2017). Therefore, L-733060 was microinjected into the RVM and found to reverse the maintenance of orofacial hyperalgesia after the EOI had been removed in the chronification stage, possibly by suppressing the facilitatory influence of ON-cells. But L-733060 did not influence either the hyperalgesia in rats with 14 d of persistent EOI or the behavior in sham rats since the ON-cells were not activated in both conditions. These findings suggest that removing the EOI in the chronification stage is too late to overcome the maintenance of hyperalgesia because of the neuroplastic transition in the RVM toward prevailing descending facilitation.

Similarly, altered functioning of brainstem pain-modulation systems has also been shown to contribute to the maintenance of chronic pain in clinical studies through the use of resting-state functional magnetic resonance imaging in humans (Mills et al., 2018; Napadow et al., 2019). Male and female patients with chronic neuropathic orofacial pain following nerve injury show increased functional connectivity between the RVM and other brainstem pain-modulatory regions, including the ventrolateral PAG and locus coeruleus. In addition, an increase in RVM functional connectivity with the spinal trigeminal nucleus was also identified (Mills et al., 2018).

Some limitations of the present study should be noted. We did not test the effects of opioid and NK-1 processes directly on ON-cells and OFF-cells in our models, although these effects were proved *in vitro* or *in vivo* in several other studies (see above). We also did not record orofacial afferents to show directly that EOI removal, or indeed its placement, was associated with decreased or increased nociceptive afferent inputs, respectively. However, these changes are likely to have occurred since a previous study demonstrated increased expression of nociceptive receptors in the trigeminal ganglion induced by EOI (Xu et al., 2016). Future research could also focus on the spatiotemporal control of pain-modulating RVM circuits by manipulation of the two major neuron populations in the RVM and on exploring further the neuroplastic changes within these circuits by manipulating peripheral inputs.

The present results indicate that EOI elicits time-dependent orofacial mechanical hyperalgesia, and EOI removal in the initial stage but not in the chronification stage can reverse the hyperalgesia in male rats. The findings also reveal that these outcomes may be modulated by adaptive changes in descending inhibitory and facilitatory influences from the RVM. The findings especially bear on the transition from acute to chronic pain following injury and therefore highlight the necessity of early intervention

to address the possibility of maintenance of chronic pain resulting from the EOI.

References

Abd-Elsayed AA, Ikeda R, Jia Z, Ling J, Zuo X, Li M, Gu JG (2015) KCNQ channels in nociceptive cold-sensing trigeminal ganglion neurons as therapeutic targets for treating orofacial cold hyperalgesia. Mol Pain 11:45–45.

Ackley MA, Hurley RW, Virnich DE, Hammond DL (2001) A cellular mechanism for the antinociceptive effect of a kappa opioid receptor agonist. Pain 91:377–388.

Ahn D, Lim E, Kim B, Yang G, Lee M, Ju J, Han S, Bae Y (2009) Compression of the trigeminal ganglion produces prolonged nociceptive behavior in rats. Eur J Pain 13:568–575.

Bagley EE, Ingram SL (2020) Endogenous opioid peptides in the descending pain modulatory circuit. Neuropharmacology 173:108131.

Bardin L (2011) The complex role of serotonin and 5-HT receptors in chronic pain. Behav Pharmacol 22:390–404.

Bodnar R, Heinricher MM (2016) Central mechanisms of pain suppression: central mechanisms of pain modulation. In: Neuroscience in the 21st century: from basic to clinical (Pfaff DW, Volkow ND, eds), pp 3439–3464. New York: Springer New York.

Bryan C, Guo W, Wei F, Yu P, Ronald D, Ren K (2012) Trigeminal-rostral ventromedial medulla circuitry is involved in orofacial hyperalgesia contralateral to tissue injury. Mol Pain 8:78–89.

Burgess SE, Gardell LR, Ossipov MH, Malan TP, Vanderah TW, Lai J, Porreca F (2002) Time-dependent descending facilitation from the rostral ventromedial medulla maintains, but does not initiate, neuropathic pain. J Neurosci 22:5129–5136.

Cao Y, Xie QF, Li K, Light AR, Fu KY (2009) Experimental occlusal interference induces long-term masticatory muscle hyperalgesia in rats. Pain 144:287–293.

Cao Y, Wang H, Chiang C-Y, Dostrovsky JO, Sessle BJ (2013a) Pregabalin suppresses nociceptive behavior and central sensitization in a rat trigeminal neuropathic pain model. J Pain 14:193–204.

Cao Y, Li K, Fu KY, Xie QF, Chiang CY, Sessle BJ (2013b) Central sensitization and MAPKs are involved in occlusal interference-induced facial pain in rats. J Pain 14:793–807.

Carlson JD, Maire JJ, Martenson ME, Heinricher MM (2007) Sensitization of pain-modulating neurons in the rostral ventromedial medulla after peripheral nerve injury. J Neurosci 27:13222–13231.

Cha M, Kohan KJ, Zuo X, Ling JX, Gu JG (2012) Assessment of chronic trigeminal neuropathic pain by the orofacial operant test in rats. Behav Brain Res 234:82–90.

Chai B, Guo W, Wei F, Dubner R, Ren K (2012) Trigeminal-rostral ventromedial medulla circuitry is involved in orofacial hyperalgesia contralateral to tissue injury. Mol Pain 8:78.

Chiang CY, Li Z, Dostrovsky JO, Sessle BJ (2010) Central sensitization in medullary dorsal horn involves gap junctions and hemichannels. Neuroreport 21:233–237.

Chichorro JG, Porreca F, Sessle B (2017) Mechanisms of craniofacial pain. Cephalalgia 37:613–626.

Chung MK, Wang S, Yang J, Alshanqiti I, Wei F, Ro JY (2020) Neural pathways of craniofacial muscle pain: implications for novel treatments. J Dent Res 99:1004–1012.

Cleary DR, Heinricher MM (2013) Adaptations in responsiveness of brainstem pain-modulating neurons in acute compared with chronic inflammation. Pain 154:845–855.

Dénes B, Khasabov SG, Mantyh PW, Simone DA (2007) NK-1 receptors modulate the excitability of ON cells in the rostral ventromedial medulla. J Neurophysiol 97:1388–1395.

De Felice M, Sanoja R, Wang R, Vera-Portocarrero L, Oyarzo J, King T, Ossipov MH, Vanderah TW, Lai J, Dussor GO, Fields HL, Price TJ, Porreca F (2011) Engagement of descending inhibition from the rostral ventromedial medulla protects against chronic neuropathic pain. Pain 152:2701–2709.

Fields H (2004) State-dependent opioid control of pain. Nat Rev Neurosci 5:565–575.

Foo H, Helmstetter FJ (2000) Activation of kappa opioid receptors in the rostral ventromedial medulla blocks stress-induced antinociception. Neuroreport 11:3349–3352.

Gonçalves L, Almeida A, Pertovaara A (2007) Pronociceptive changes in response properties of rostroventromedial medullary neurons in a rat model of peripheral neuropathy. Eur J Neurosci 26:2188–2195.

Heinricher MM, Barbaro NM, Fields HL (1989) Putative nociceptive modulating neurons in the rostral ventromedial medulla of the rat: firing of on- and off-cells is related to nociceptive responsiveness. Somatosens Mot Res 6:427–439.

Heinricher MM, Tavares I, Leith JL, Lumb BM (2009) Descending control of nociception: specificity, recruitment and plasticity. Brain Res Rev 60:214–225.

Iwata K, Sessle BJ (2019) The evolution of neuroscience as a research field relevant to dentistry. J Dent Res 98:1407–1417.

Iwata K, Imamura Y, Honda K, Shinoda M (2011) Physiological mechanisms of neuropathic pain: the orofacial region. Int Rev Neurobiol 97:227–250.

Khasabov SG, Brink TS, Schupp M, Noack J, Simone DA (2012) Changes in response properties of rostral ventromedial medulla neurons during prolonged inflammation: modulation by neurokinin-1 receptors. Neuroscience 224:235–248.

Khasabov SG, Malecha P, Noack J, Tabakov J, Okamoto K, Bereiter DA, Simone DA (2015) Activation of rostral ventromedial medulla neurons by noxious stimulation of cutaneous and deep craniofacial tissues. J Neurophysiol 113:14–22.

Khasabov SG, Malecha P, Noack J, Tabakov J, Giesler GJ Jr, Simone DA (2017) Hyperalgesia and sensitization of dorsal horn neurons following activation of NK-1 receptors in the rostral ventromedial medulla. J Neurophysiol 118:2727–2744.

Kong J, Yang Y, Sun S, Xie J, Lin X, Ji P (2016) Effect of toll-like receptor 4 on synovial injury of temporomandibular joint in rats caused by occlusal interference. Mediators Inflamm 2016:7694921.

Kwon M, Altin M, Duenas H, Alev L (2014) The role of descending inhibitory pathways on chronic pain modulation and clinical implications. Pain Pract 14:656–667.

Li XJ, Cao Y, Xie QF (2014) Characteristics of experimental occlusal interference-induced masticatory mechanical hyperalgesia of rats. Chin J Stomatol 49:596–599.

Lin X, Xie J, Sun S, Ren X, Kong J, Ji P (2018) Toll-like receptor 4 (TLR4) stimulates synovial injury of temporomandibular joint in rats through the activation of p38 mitogen-activated protein kinase (MAPK) signaling pathway. Med Sci Monit 24:4405–4412.

Liu CR, Xu XX, Cao Y, Xie QF (2016) Influence of the occlusal interference time on masticatory muscle mechanical hyperalgesia in rats. J Peking Univ Health Sci 48:51–56.

López-Avila A, Coffeen U, Ortega-Legaspi JM, del Ángel R, Pellicer F (2004) Dopamine and NMDA systems modulate long-term nociception in the rat anterior cingulate cortex. Pain 111:136–143.

Martins I, Tavares I (2017) Reticular formation and pain: the past and the future. Front Neuroanat 11:51.

Meng ID, Johansen JP, Harasawa I, Fields HL (2005) Kappa opioids inhibit physiologically identified medullary pain modulating neurons and reduce morphine antinociception. J Neurophysiol 93:1138–1144.

Mills EP, Di Pietro F, Alshelh Z, Peck CC, Murray GM, Vickers ER, Henderson LA (2018) Brainstem pain-control circuitry connectivity in chronic neuropathic pain. J Neurosci 38:465–473.

Napadow V, Sclocco R, Henderson LA (2019) Brainstem neuroimaging of nociception and pain circuitries. Pain Rep 4:e745.

Nones CFM, Claudino RF, Ferreira LEN, Reis RCD, King T, Chichorro JG (2017) Descending facilitatory pain pathways mediate ongoing pain and tactile hypersensitivity in a rat model of trigeminal neuropathic pain. Neurosci Lett 644:18–23.

Okubo M, Castro A, Guo W, Zou S, Ren K, Wei F, Keller A, Dubner R (2013) Transition to persistent orofacial pain after nerve injury involves supraspinal serotonin mechanisms. J Neurosci 33:5152–5161.

Ossipov MH (2009) Pain pathways: descending modulation. In: Encyclopedia of neuroscience (Squire LR, ed), pp 393–399. Oxford, UK: Academic.

Ossipov MH, Dussor GO, Porreca F (2010) Central modulation of pain. J Clin Invest 120:3779–3787.

Ossipov MH, Morimura K, Porreca F (2014) Descending pain modulation and chronification of pain. Curr Opin Support Palliat Care 8:143–151.

Pacharinsak C, Khasabov SG, Beitz AJ, Simone DA (2008) NK-1 receptors in the rostral ventromedial medulla in hyperalgesia produced by intraplantar injection of capsaicin. Pain 139:34–46.

Pan ZZ, Tershner SA, Fields HL (1997) Cellular mechanism for anti-analgesic action of agonists of the kappa-opioid receptor. Nature 389:382–385.

Paxinos G, Watson C (2009) The rat brain in stereotaxic coordinates, Ed 6. San Diego, CA: Academic.

Porreca F, Burgess SE, Gardell LR, Vanderah TW, Malan TP Jr, Ossipov MH, Lappi DA, Lai J (2001) Inhibition of neuropathic pain by selective ablation of brainstem medullary cells expressing the μ-opioid receptor. J Neurosci 21:5281–5288.

Porreca F, Ossipov MH, Gebhart GF (2002) Chronic pain and medullary descending facilitation. Trends Neurosci 25:319–325.

Qi D, Yang Y, Ji P, Kong J, Wu Q, Si H (2016) Upregulation of the purinergic receptor subtype P2X3 in the trigeminal ganglion is involved in orofacial pain induced by occlusal interference in rats. J Oral Facial Pain Headache 30:51–60.

Ren K, Dubner R (2002) Descending modulation in persistent pain: an update. Pain 100:1–6.

Ren K, Dubner R (2011) The role of trigeminal interpolaris-caudalis transition zone in persistent orofacial pain. Int Rev Neurobiol 97:207–225.

Salas MM, Hargreaves KM, Akopian AN (2009) TRPA1-mediated responses in trigeminal sensory neurons: interaction between TRPA1 and TRPV1. Eur J Neurosci 29:1568–1578.

Salas R, Ramirez K, Vanegas H, Vazquez E (2016) Activity correlations between on-like and off-like cells of the rostral ventromedial medulla and simultaneously recorded wide-dynamic-range neurons of the spinal dorsal horn in rats. Brain Res 1652:103–110.

Sessle BJ (2021) Chronic orofacial pain: models, mechanisms, and genetic and related environmental influences. Int J Mol Sci 22:7112–7139.

Sessle BJ, Hu JW, Dubner R, Lucier GE (1981) Functional properties of neurons in cat trigeminal subnucleus caudalis (medullary dorsal horn). II. Modulation of responses to noxious and nonnoxious stimuli by periaqueductal gray, nucleus raphe magnus, cerebral cortex, and afferent influences, and effect of naloxone. J Neurophysiol 45:193–207.

Shimizu K, Chai B, LaGraize SC, Wei F, Dubner R, Ren K (2009) Microinjection of IL-1β into the trigeminal transition zone produces bilateral NMDA receptor-dependent orofacial hyperalgesia involving descending circuitry. Open Pain J 2:76–83.

Shinoda M, Hayashi Y, Kubo A, Iwata K (2020) Pathophysiological mechanisms of persistent orofacial pain. J Oral Sci 62:131–135.

Silva M, Amorim D, Almeida A, Tavares I, Pinto-Ribeiro F, Morgado C (2013) Pronociceptive changes in the activity of rostroventromedial medulla (RVM) pain modulatory cells in the streptozotocin-diabetic rat. Brain Res Bull 96:39–44.

Simonic-Kocijan S, Zhao X, Liu W, Wu Y, Uhac I, Wang KW (2013) TRPV1 channel-mediated bilateral allodynia induced by unilateral masseter muscle inflammation in rats. Mol Pain 9:68.

Sugiyo S, Takemura M, Dubner R, Ren K (2005) Trigeminal transition zone/rostral ventromedial medulla connections and facilitation of orofacial hyperalgesia after masseter inflammation in rats. J Comp Neurol 493:510–523.

Sun S, Qi D, Yang Y, Ji P, Kong J, Wu Q (2016) Association of occlusal interference-induced masseter muscle hyperalgesia and P2X3 receptors in the trigeminal subnucleus caudalis and midbrain periaqueductal gray. Neuroreport 27:277–283.

Suzuki R, Rygh LJ, Dickenson AH (2004) Bad news from the brain: descending 5-HT pathways that control spinal pain processing. Trends Pharmacol Sci 25:613–617.

Takahashi K, Taguchi T, Itoh K, Okada K, Kawakita K, Mizumura K (2005) Influence of surface anesthesia on the pressure pain threshold measured with different-sized probes. Somatosens Mot Res 22:299–305.

Tang J-S, Chiang CY, Dostrovsky JO, Yao D, Sessle BJ (2021) Responses of neurons in rostral ventromedial medulla to nociceptive stimulation of craniofacial region and tail in rats. Brain Res 1767:147539–147549.

Terayama R, Guan Y, Dubner R, Ren K (2000) Activity-induced plasticity in brain stem pain modulatory circuitry after inflammation. Neuroreport 11:1915–1919.

Wang H, Cao Y, Chiang C-Y, Dostrovsky JO, Sessle BJ (2014) The gap junction blocker carbenoxolone attenuates nociceptive behavior and medullary dorsal horn central sensitization induced by partial infraorbital nerve transection in rats. Pain 155:429–435.

Winkler CW, Hermes SM, Chavkin CI, Drake CT, Morrison SF, Aicher SA (2006) Kappa opioid receptor (KOR) and GAD67 immunoreactivity are found in OFF and NEUTRAL cells in the rostral ventromedial medulla. J Neurophysiol 96:3465–3473.

Xu XX, Cao Y, Ding TT, Fu KY, Li Y, Xie QF (2016) Role of TRPV1 and ASIC3 channels in experimental occlusal interference-induced hyperalgesia in rat masseter muscle. Eur J Pain 20:552–563.

Xu XX, Cao Y, Mo SY, Liu Y, Xie QF (2019) ACC plasticity maintains masseter hyperalgesia caused by occlusal interference. J Dent Res 98:589–596.